Kragujevac Journal of Mathematics
Volume 51(7) (2027), Pages 1159–1193.

NUMERICAL AND ANALYTICAL INVESTIGATION FOR INVERSE COEFFICIENT NON-LINEAR PSEUDO-HYPERBOLIC EQUATION WITH PERIODIC BOUNDARY CONDITION

AKBALA YERNAZAR[1], ERMAN ASLAN[2,*], AND IREM BAĞLAN[1]

Abstract. This research delves into an inverse problem concerning time-dependent coefficients in a one-dimensional nonlinear pseudo-hyperbolic equation subject to periodic boundary conditions. Employing the generalized Fourier method, we construct Fourier coefficients for the solutions. Through iterative convergence analysis, we establish the uniqueness and stability of solutions to the nonlinear problem. Furthermore, to tackle the inverse problem numerically, we propose employing the implicit Finite Difference Method (FDM). Two finite difference equations are formulated and solved with different accuracies. In the first equation, a first-order accurate time discretization is used, and second-order accurate finite difference equations are employed for spatial and multi-variable partial differential equation discretization. In the second equation, a second-order accurate time discretization is applied, and fourth-order accurate finite difference equations are utilized for the discretization of spatial and multi-variable partial differential equations. At a specific time, the w value appears as a hyperbolic curve with one negative peak and one positive peak. However, in terms of the estimated w value, the difference between two different accurate schemes is minimal, and these values align with the real values. Additionally, the finite-difference scheme with higher accuracy provides a better estimation of the inverse coefficient.

1. Introduction

Partial differential equations (PDEs) constitute a fundamental area of applied mathematics in many scientific and engineering disciplines. Hyperbolic equations,

Key words and phrases. Inverse Coefficient Problem, Nonlinear Pseudo-Hyperbolic Equation, Nonlocal Boundary Condition, Fourier Method, Finite Difference Method.

2020 *Mathematics Subject Classification.* Primary: 35R30. Secondary: 65M06, 35A01, 35A02.

DOI

Received: September 03, 2024.

Accepted: April 25, 2026.

commonly referred to as wave equations, describe the propagation of waves and vibrations within a medium [1, 2]. These equations play a central role in vibration analysis for predicting and controlling mechanical oscillations in engineering systems [3]. In thermal engineering, the heat conduction equation, considered a variant of the wave equation, governs the propagation of thermal waves and provides insight into heat transfer mechanisms [4]. In fluid mechanics, wave equations are used to analyze acoustic wave propagation and fluid-acoustic interactions [5]. They also applied in material science to investigate electromagnetic wave dispersion in advanced materials [6], in control engineering for modeling and analyzing dynamic systems [7], and in robotics for the design of wave-based sensors and actuators [8].

A simple yet illustrative demonstration of hyperbolic equations in one dimension is depicted by the motion of a spring in a prescribed direction. Extending into two dimensions, envision a guitarist plucking a guitar string, the vibrations of which exemplify this concept further. Advancing into the realm of three dimensions, contemplate a scenario where dispersed particles collide with a specific location, showcasing the intricate dynamics governed by hyperbolic equations. In each case, the unmistakable trend emerges as the wave motions gradually dissipate over time, succumbing to the influence of frictional forces inherent in the system. Moreover, the significance of hyperbolic equations transcends these tangible examples, finding widespread utility in diverse fields. In atmospheric fluid dynamics, they serve as indispensable tools for modeling intricate weather phenomena. Similarly, in the realm of pollutant dispersion within porous mediums, these equations offer crucial insights into the complex transport mechanisms at play. Furthermore, hyperbolic equations play a pivotal role in understanding aerodynamic flows, guiding the design and optimization of various aerospace systems. Beyond these applications, they also underpin the fundamental principles governing signal propagation, crucial for telecommunications and information technology [2].

The endeavor of determining the coefficients of the source function within a differential equation, while considering initial or boundary conditions and incorporating an additional condition given for the solution, constitutes what is known as an inverse problem. These intriguing challenges arise across a multitude of disciplines, spanning the realms of natural science, environmental pollution assessment, medical imaging such as computerized tomography, seismology in earthquake science, as well as the precise identification of the location and quantity of valuable underground resources. Moreover, they play a crucial role in examining regional infrastructure, leveraging satellite information to analyze and optimize various aspects of infrastructure development and maintenance. The breadth of applications underscores the significance and interdisciplinary nature of inverse problems, highlighting their pervasive presence and importance in addressing real-world complexities and uncertainties [9].

In modern scientific and technical domains, the utility of inverse problems extends to determining parameters that elude direct calculation, thus igniting a surge of interest in this field during the mid-20th century. Since then, it has remained a

vibrant area of inquiry, constantly evolving to meet the demands of contemporary research and applications. The practical significance of inverse problems positions them at the forefront of modern mathematics, playing a pivotal role in elucidating crucial properties of various mediums. These properties encompass a wide array of factors, including but not limited to wavelength intensity, velocity profiles, elasticity characteristics, conductivity behavior, as well as electric and magnetic permeability coefficients. Moreover, inverse problems enable the identification and characterization of inhomogeneities within inaccessible regions, offering invaluable insights into the structure and composition of complex systems. Of particular note is the relevance of inverse problems in seismology, where they hold special significance for understanding seismic wave propagation and interpreting geological structures. Through the lens of hyperbolic/wave equations, these problems provide indispensable tools for seismic analysis, aiding in the exploration of subsurface geology, detection of seismic hazards, and assessment of earthquake risk. In essence, the enduring relevance and interdisciplinary nature of inverse problems underscore their critical role in advancing scientific understanding and technological innovation across a myriad of fields [10-17].

The resolution of such problems is notably affected by the imposition of boundary conditions, with nonlocal conditions presenting significant challenges in their treatment [17]. Nonlocal problems have garnered considerable attention in contemporary physics, biology, chemistry, and engineering, particularly in scenarios where determining boundary values of the unknown function is unfeasible. Among these nonlocal conditions, periodic boundary conditions stand out for their versatility and applicability across diverse problem domains [17-20]. Periodic boundary conditions, a subtype of nonlocal conditions, have found wide-ranging use in scientific investigations. For instance, in lunar theory, they are instrumental in examining the mobility of the moon, offering insights into celestial mechanics [18]. Similarly, in molecular dynamics and fluid dynamics simulations, periodic boundary conditions prove invaluable for addressing cyclically repetitive scenarios, enabling researchers to model complex systems with greater accuracy and efficiency.

The Fourier method stands out as a versatile and powerful technique for tackling nonlinear inverse coefficient problems, showcasing its efficacy in establishing the existence, uniqueness, convergence, and stability of solutions across a spectrum of nonlinear hyperbolic and parabolic equations. It's worth emphasizing that the utility of the Fourier method transcends hyperbolic equations, finding applicability in a myriad of other equation types, including but not limited to the Euler-Bernoulli, Heat, Burger, and Klein-Gordon equations, all with periodic boundary conditions. Moreover, the method's broad scope has prompted numerous researchers to delve into the exploration of inverse coefficient hyperbolic equations, employing a diverse array of methodologies. This ongoing exploration underscores the method's enduring relevance and the continuous evolution of techniques for addressing complex mathematical challenges in various scientific and engineering disciplines.

In addressing the challenge posed by the one-dimensional wave equation with an inverse coefficient problem, researchers have explored a multitude of numerical methods to obtain accurate solutions. Among these methods, the finite difference method [21, 22], finite element methods [23-25], and finite volume methods [26-32] in a quite wide range of applications. have emerged as prominent choices. Anne et al. delved into both analytical and numerical approaches to tackle the one-dimensional wave equation [33]. They employed advanced higher-order finite difference schemes in their numerical solutions, demonstrating a meticulous approach to achieving accurate results. In a similar vein, Wang et al. utilized the finite difference method to address the complexities of the two-dimensional wave equation [34]. Their study began with the establishment of a comprehensive framework for analyzing convergence in one-dimensional problems, which they later extended to encompass two-dimensional scenarios. The numerical solutions obtained through their methodology exhibited a high degree of accuracy. Liu and Guo introduced a new space semidiscretized finite difference scheme for approximating the one-dimensional wave equation with boundary feedback. This scheme, known as the order reduction finite difference scheme, maintains uniform exponential stability without the need for numerical viscosity [35]. Madaliev et al. had compared first, second and third order-accurate finite difference schems in soliving the one and tw0-dimensionla wave equation [36]. Silva Jr. et al. contributed to the field by addressing the numerical solution of the one-dimensional nonlinear wave equation [37]. Their approach involved the utilization of regressive and central differences of varying orders, coupled with various refinement techniques during numerical simulations. Through their meticulous efforts, they proposed a formulation that yielded highly satisfactory results, further enriching the repertoire of techniques available for solving such intricate problems. In addition, analytical and numerical solutions of pseudo-parabolic equations are available in the literature[38-41].

In this current study, we delve into an inverse problem involving unknown time-dependent coefficients in a one-dimensional nonlinear pseudo-hyperbolic equation with periodic boundary conditions. Employing the Fourier method for analytical solutions, we generate Fourier coefficients and establish the convergence, uniqueness, and stability of the solution through an iterative approach. Two finite-difference equations have been developed and solved with varying levels of accuracy. The first equation incorporates a first-order accurate time discretization, coupled with second-order accurate finite difference equations for the discretization of spatial and multi-variable partial differential equations. In the second equation, a second-order accurate time discretization is implemented, and fourth-order accurate finite difference equations are utilized for the discretization of spatial and multi-variable partial differential equations. The originality of this work lies in the analytical solution of the pseudo-hyperbolic equation using the Fourier method under periodic boundary conditions, as well as its numerical solution via the finite difference method. Furthermore, the use of two finite difference schemes with different orders of accuracy and their comparative evaluation constitutes another novel aspect of this study.

2. Solution of a Problem

For $T > 0$ in the domain $\Omega := \{0 < x < \pi,\ 0 < t < T\}$, we set following pseudo-hyperbolic problem

$$w_{tt} - \varepsilon w_{xxtt} - w_{xx} = s(t) f(x,t,w), \tag{2.1}$$

with initial data

$$\begin{aligned} w(x,0,\varepsilon) =& \varphi(x), \\ w_t(x,0,\varepsilon) =& \psi(x), \end{aligned} \tag{2.2}$$

periodic boundary conditions

$$\begin{aligned} w(0,t,\varepsilon) =& w(\pi,t,\varepsilon), \\ w_x(0,t,\varepsilon) =& w_x(\pi,t,\varepsilon), \end{aligned} \tag{2.3}$$

and overdetermination condition

$$E(t,\varepsilon) = \int_0^\pi x w(x,t,\varepsilon) dx, \tag{2.4}$$

where ϕ, ψ, E are specified functions.

The problem of identifying the pair $\{s(t),\ w(x,t)\}$ in (2.1)–(2.4) is referred to as an inverse problem. B is termed a Banach space when the following set

$$\{w(t)\} = \{w_0(t),\ w_{ck}(t),\ w_{sk}(t),\ k = 1,2,3,\dots\}$$

of continuous on [0,T] functions satisfying the norm

$$\|w(t)\| = \max_{0\le t\le T} |w_0(t)| + \sum_{k=1}^{+\infty} \left(\max_{0\le t\le T} |w_{ck}(t)| + \max_{0\le t\le T} |w_{sk}(t)| \right).$$

Since a Banach space contains all its limit points, working within this space facilitates handling more extensive operations.

Let's establish the following assumptions regarding the data of problem (2.1)–(2.4)

(A1) $E(t) \in C^2[0,T]$, $s(t) \in C[0,T]$,

(A2) $\varphi(x) \in C^1[0,\pi]$, $\psi(x) \in C^1[0,\pi]$.

(A3) Assume that the function $f(x,t,w)$ remains continuous across all arguments in $\Omega \times (-\infty, +\infty)$ and satisfies the subsequent condition:

$$\left| \frac{\partial^{(k)} f(x,t,w)}{\partial x^{(k)}} - \frac{\partial^{(k)} f(x,t,\tilde{w})}{\partial x^{(k)}} \right| \le b(x,t) \left| w - \tilde{w} \right|, \quad k = \overline{0,2},$$

where $b(x,t) \in L_2(\Omega)$, $b(x,t) \ge 0$, $f(x,t,w) \in C^1[0,\pi]$, $t \in [0,\ T]$, $|f(x,t,w)| \le M$, $\int_0^\pi f(x,t,w)dx \ne 0$ for all $t \in [0,T]$.

Using the Fourier Method, we acquire the solution for (2.1)–(2.3) as follows:

$$w(x,t,\varepsilon) = \frac{1}{2} \left(\varphi_0 + \psi_0 t + \frac{2}{\pi} \int_0^t \int_0^\pi s(\tau)(t-\tau) f(\xi,\tau,w) d\xi d\tau \right) \tag{2.5}$$

$$+\sum_{k=1}^{+\infty}\left(\varphi_{ck}\cos\alpha_k t+\frac{1}{\alpha_k}\psi_{ck}\sin\alpha_k t\right.$$
$$\left.+\frac{1}{\alpha_k}\cdot\frac{2}{\pi}\int_0^t\int_0^\pi s(\tau)f(\xi,\tau,w)\cos 2k\xi\sin\alpha_k(t-\tau)d\xi d\tau\right)\cos 2kx$$
$$+\sum_{k=1}^{+\infty}\left(\varphi_{sk}\cos\alpha_k t+\frac{1}{\alpha_k}\psi_{sk}\sin\alpha_k t\right.$$
$$\left.+\frac{1}{\alpha_k}\cdot\frac{2}{\pi}\int_0^t\int_0^\pi s(\tau)f(\xi,\tau,w)\sin 2k\xi\sin\alpha_k(t-\tau)d\xi d\tau\right)\sin 2kx,$$

where $\alpha_k=\frac{2k}{\sqrt{1+4\varepsilon k^2}}$. Subject to conditions (A1)-(A3), upon differentiation of (2.4)

$$E''(t,\varepsilon)=\int_0^\pi xw_{tt}(x,t,\varepsilon)dx, \tag{2.6}$$

and using the initial data (2.2), (2.5)–(2.6), we obtain

$$s(t)=\frac{E''(t,\varepsilon)+\varepsilon\psi_t(\pi)-\varepsilon\psi_t(0)}{\int_0^\pi xf(x,t,w)dx}$$
$$-\frac{\pi\sum_{k=1}^{+\infty}(2k)\left(\left(1-\varepsilon\alpha_k^2\right)\varphi_{sk}\cos\alpha_k t+\left(\frac{1}{\alpha_k}-\varepsilon\alpha_k\right)\psi_{sk}\sin\alpha_k t+\frac{1}{\alpha_k}\int_0^t s(\tau)f_{sk}(\tau,w)\sin\alpha_k(t-\tau)d\tau\right)}{\int_0^\pi xf(x,t,w)dx}. \tag{2.7}$$

3. Existence and Uniqueness of the Solution of the Inverse Problem

Theorem 3.1. *If the assumptions* (A1)-(A3) *are satisfied, then* (2.1)–(2.4) *possess a singular or one solution.*

Proof. Iteration for Fourier coefficients of (2.5) are:

$$w_0^{(N+1)}(t,\varepsilon)=w_0^{(0)}(t,\varepsilon)+\frac{2}{\pi}\int_0^t\int_0^\pi s^{(N)}(\tau)(t-\tau)f(\xi,\tau,w^{(N)})d\xi d\tau,$$
$$w_{ck}^{(N+1)}(t,\varepsilon)=w_{ck}^{(0)}(t,\varepsilon)+\frac{1}{\alpha_k}\cdot\frac{2}{\pi}\int_0^t\int_0^\pi s^{(N)}(\tau)f(\xi,\tau,w^{(N)})\cos 2k\xi\sin\alpha_k(t-\tau)d\xi d\tau,$$
$$w_{sk}^{(N+1)}(t,\varepsilon)=w_{sk}^{(0)}(t,\varepsilon)+\frac{1}{\alpha_k}\cdot\frac{2}{\pi}\int_0^t\int_0^\pi s^{(N)}(\tau)f(\xi,\tau,w^{(N)})\sin 2k\xi\sin\alpha_k(t-\tau)d\xi d\tau,$$

where

$$w_0^{(0)}(t,\varepsilon)=\varphi_0+\psi_0 t,$$
$$w_{ck}^{(0)}(t,\varepsilon)=\varphi_{ck}\cos\alpha_k t+\frac{1}{\alpha_k}\psi_{ck}\sin\alpha_k t,$$

$$w_{sk}^{(0)}(t,\varepsilon) = \varphi_{sk}\cos\alpha_k t + \frac{1}{\alpha_k}\psi_{sk}\sin\alpha_k t,$$

$w^{(0)}(t) \in B$, $t \in [0,T]$, is from the conditions of the theorem. We prove that subsequent approximations also fulfill this condition through our proof. Let us analyze the Fourier coefficients for $N = 0$:

$$w_0^{(1)}(t,\varepsilon) = \varphi_0 + \psi_0 t + \frac{2}{\pi}\int_0^t\int_0^\pi s^{(0)}(\tau)(t-\tau)f(\xi,\tau,w^{(0)})\,d\xi\,d\tau,$$

$$\begin{aligned} w_{ck}^{(1)}(t,\varepsilon) &= \varphi_{ck}\cos\alpha_k t + \frac{\psi_{ck}}{\alpha_k}\sin\alpha_k t \\ &\quad + \frac{1}{\alpha_k}\cdot\frac{2}{\pi}\int_0^t\int_0^\pi s^{(0)}(\tau)f(\xi,\tau,w^{(0)})\cos 2k\xi\sin\alpha_k(t-\tau)\,d\xi\,d\tau, \end{aligned}$$

$$\begin{aligned} w_{sk}^{(1)}(t,\varepsilon) &= \varphi_{sk}\cos\alpha_k t + \frac{\psi_{sk}}{\alpha_k}\sin\alpha_k t \\ &\quad + \frac{1}{\alpha_k}\cdot\frac{2}{\pi}\int_0^t\int_0^\pi s^{(0)}(\tau)f(\xi,\tau,w^{(0)})\sin 2k\xi\sin\alpha_k(t-\tau)\,d\xi\,d\tau. \end{aligned}$$

By adding and subtracting the integral $\int\limits_0^t\int\limits_0^\pi f(\xi,\tau,0)d\xi d\tau$ to the right-hand sides of the equations, taking the absolute value, we obtain

$$\begin{aligned} \left|w_0^{(1)}(t)\right| &\le |\varphi_0| + |\psi_0 t| + \left|\frac{2}{\pi}\int\limits_0^t\int\limits_0^\pi s^{(0)}(\tau)f(\xi,\tau,0)(t-\tau)d\xi d\tau\right| \\ &\quad + \left|\frac{2}{\pi}\int\limits_0^t\int\limits_0^\pi s^{(0)}(\tau)(t-\tau)\left[f(\xi,\tau,w^{(0)}) - f(\xi,\tau,0)\right]d\xi d\tau\right|, \\ \left|w_{ck}^{(1)}(t)\right| &\le \sum_{k=1}^{+\infty}|\varphi_{ck}| + \sum_{k=1}^{+\infty}\left|\frac{\psi_{ck}}{\alpha_k}\right| \\ &\quad + \sum_{k=1}^{+\infty}\left|\frac{1}{\alpha_k}\cdot\frac{2}{\pi}\int\limits_0^t\int\limits_0^\pi s^{(0)}(\tau)f(\xi,\tau,0)\cos 2k\xi\sin\alpha_k(t-\tau)d\xi d\tau\right| \\ &\quad + \sum_{k=1}^{+\infty}\left|\frac{1}{\alpha_k}\cdot\frac{2}{\pi}\int\limits_0^t\int\limits_0^\pi s^{(0)}(\tau)\left[f(\xi,\tau,w^{(0)}) - f(\xi,\tau,0)\right]\cos 2k\xi\sin\alpha_k(t-\tau)d\xi d\tau\right|, \\ \left|w_{sk}^{(1)}(t)\right| &\le \sum_{k=1}^{+\infty}|\varphi_{sk}| + \sum_{k=1}^{+\infty}\left|\frac{\psi_{sk}}{\alpha_k}\right| \\ &\quad + \sum_{k=1}^{+\infty}\left|\frac{1}{\alpha_k}\cdot\frac{2}{\pi}\int\limits_0^t\int\limits_0^\pi s^{(0)}(\tau)f(\xi,\tau,0)\sin 2k\xi\sin\alpha_k(t-\tau)d\xi d\tau\right| \\ &\quad + \sum_{k=1}^{+\infty}\left|\frac{1}{\alpha_k}\cdot\frac{2}{\pi}\int\limits_0^t\int\limits_0^\pi s^{(0)}(\tau)\left[f(\xi,\tau,w^{(0)}) - f(\xi,\tau,0)\right]\sin 2k\xi\sin\alpha_k(t-\tau)d\xi d\tau\right|. \end{aligned}$$

Apllying Cauchy inequality, we have

$$\left|w_0^{(1)}(t)\right| \le |\varphi_0| + |\psi_0 t| + \left(\int_0^t (t-\tau)^2 d\tau\right)^{\frac{1}{2}} \left(\int_0^t \left(\frac{2}{\pi}\int_0^\pi s^{(0)}(\tau) f(\xi,\tau,0) d\xi\right)^2 d\tau\right)^{\frac{1}{2}}$$
$$+ \left(\int_0^t (t-\tau)^2 d\tau\right)^{\frac{1}{2}} \left(\int_0^t \left(\frac{2}{\pi}\int_0^\pi s^{(0)}(\tau)\left[f(\xi,\tau,w^{(0)}) - f(\xi,\tau,0)\right] d\xi\right)^2 d\tau\right)^{\frac{1}{2}},$$

$$\left|w_{ck}^{(1)}(\psi)\right| \le \sum_{k=1}^{+\infty} |\varphi_{ck}| + \sum_{k=1}^{+\infty} \left|\frac{\psi_{ck}}{\alpha_k}\right| + \sum_{k=1}^{+\infty} \frac{1}{\alpha_k}\left(\int_0^t d\tau\right)^{\frac{1}{2}}$$
$$\times \left(\int_0^t \left(\frac{2}{\pi}\int_0^\pi s^{(0)}(\tau) f(\xi,\tau,0)\cos 2k\xi \sin\alpha_k(t-\tau) d\xi\right)^2 d\tau\right)^{\frac{1}{2}} + \sum_{k=1}^{+\infty} \frac{1}{\alpha_k}\left(\int_0^t d\tau\right)^{\frac{1}{2}}$$
$$\times \left(\int_0^t \left(\frac{2}{\pi}\int_0^\pi s^{(0)}(\tau)\left[f(\xi,\tau,w^{(0)}) - f(\xi,\tau,0)\right]\cos 2k\xi \sin\alpha_k(t-\tau) d\xi\right)^2 d\tau\right)^{\frac{1}{2}},$$

$$\left|w_{sk}^{(1)}(\psi)\right| \le \sum_{k=1}^{+\infty} |\varphi_{sk}| + \sum_{k=1}^{+\infty} \left|\frac{\psi_{sk}}{\alpha_k}\right| + \sum_{k=1}^{+\infty} \frac{1}{\alpha_k}\left(\int_0^t d\tau\right)^{\frac{1}{2}}$$
$$\times \left(\int_0^t \left(\frac{2}{\pi}\int_0^\pi s^{(0)}(\tau) f(\xi,\tau,0)\sin 2k\xi \sin\alpha_k(t-\tau) d\xi\right)^2 d\tau\right)^{\frac{1}{2}} + \sum_{k=1}^{+\infty} \frac{1}{\alpha_k}\left(\int_0^t d\tau\right)^{\frac{1}{2}}$$
$$\times \left(\int_0^t \left(\frac{2}{\pi}\int_0^\pi s^{(0)}(\tau)\left[f(\xi,\tau,w^{(0)}) - f(\xi,\tau,0)\right]\sin 2k\xi \sin\alpha_k(t-\tau) d\xi\right)^2 d\tau\right)^{\frac{1}{2}}.$$

Applying Hölder's and Bessel's inequalities to the Fourier coefficients w_{ck} and w_{sk}, we obtain

$$\left|w_0^{(1)}(\psi)\right| \le |\varphi_0| + |\psi_0 t| + 2\sqrt{\frac{t^3}{3\pi}}\left(\int_0^t\int_0^\pi \left(s^{(0)}(\tau) f(\xi,\tau,0)\right)^2 d\xi d\tau\right)^{\frac{1}{2}}$$
$$+ 2\sqrt{\frac{t^3}{3\pi}}\left(\int_0^t\int_0^\pi \left(s^{(0)}(\tau)\left[f(\xi,\tau,w^{(0)}) - f(\xi,\tau,0)\right]\right)^2 d\xi d\tau\right)^{\frac{1}{2}},$$

$$\left|w_{ck}^{(1)}(t)\right| \le \sum_{k=1}^{+\infty} |\varphi_{ck}| + \sqrt{\frac{\pi^2}{24} + \varepsilon}\left(\sum_{k=1}^{+\infty} |\psi_{ck}|^2\right)^{\frac{1}{2}}$$

$$+2\sqrt{\frac{\pi t}{24}+\frac{\varepsilon t}{\pi}}\left(\sum_{k=1}^{+\infty}\int_0^t\int_0^\pi\left(s^{(0)}(\tau)f(\xi,\tau,0)\right)^2d\xi d\tau\right)^{\frac{1}{2}}$$

$$+2\sqrt{\frac{\pi t}{24}+\frac{\varepsilon t}{\pi}}\left(\sum_{k=1}^{+\infty}\int_0^t\int_0^\pi\left(s^{(0)}(\tau)\left[f(\xi,\tau,w^{(0)})-f(\xi,\tau,0)\right]\right)^2d\xi d\tau\right)^{\frac{1}{2}},$$

$$\left|w_{sk}^{(1)}(t)\right|\leq\sum_{k=1}^{+\infty}|\varphi_{sk}|+\sqrt{\frac{\pi^2}{24}+\varepsilon}\left(\sum_{k=1}^{+\infty}|\psi_{sk}|^2\right)^{\frac{1}{2}}$$

$$+2\sqrt{\frac{\pi t}{24}+\frac{\varepsilon t}{\pi}}\left(\sum_{k=1}^{+\infty}\int_0^t\int_0^\pi\left(s^{(0)}(\tau)f(\xi,\tau,0)\right)^2d\xi d\tau\right)^{\frac{1}{2}}$$

$$+2\sqrt{\frac{\pi t}{24}+\frac{\varepsilon t}{\pi}}\left(\sum_{k=1}^{+\infty}\int_0^t\int_0^\pi\left(s^{(0)}(\tau)\left[f(\xi,\tau,w^{(0)})-f(\xi,\tau,0)\right]\right)^2d\xi d\tau\right)^{\frac{1}{2}},$$

where $\left(\sum\limits_{k=1}^{+\infty}\frac{1}{\alpha_k^2}\right)^{\frac{1}{2}}=\sqrt{\frac{\pi^2}{24}+\varepsilon}$. Finally, applying the Lipschitz condition to all Fourier coefficients and taking the maximum over $t\in[0,T]$, we have

$$\left\|w^{(1)}(t,\varepsilon)\right\|\leq\frac{\|\varphi_0\|+\|\psi_0\|\cdot|T|}{2}+\sum_{k=1}^{+\infty}\left(\|\varphi_{ck}\|+\|\varphi_{sk}\|\right)+\sum_{k=1}^{+\infty}\left(\|\psi_{ck}\|+\|\psi_{sk}\|\right)\sqrt{\frac{\pi^2}{24}+\varepsilon}$$

$$+\left(T^2\sqrt{\frac{\pi T}{3}}+4T\sqrt{\pi T\left(\frac{\pi^2}{24}+\varepsilon\right)}\right)\left\|s^{(0)}(t)\right\|\cdot\|b(x,t)\|\cdot\left\|w^{(0)}(t,\varepsilon)\right\|$$

$$+\left(T^2\sqrt{\frac{\pi T}{3}}+4T\sqrt{\pi T\left(\frac{\pi^2}{24}+\varepsilon\right)}\right)\left\|s^{(0)}(t)\right\|\cdot\|f(x,t,0)\|.$$

Therefore, based on the conditions of the theorem, it is $w^{(1)}(t)\in B$, $t\in[0,T]$.

If

$$\int_0^\pi\varphi(x)\sin 2kxdx=\frac{1}{2k}\int_0^\pi\varphi'(x)\cos 2kxdx$$

and

$$\int_0^\pi f(x,t,w)\sin 2kxdx=\frac{1}{2k}\int_0^\pi f'(x,t,w)\cos 2kxdx$$

are taken into account for the inverse coefficient, the formulation of (2.7) will be

(3.1)

$$s(t)=\frac{E''(t)+\varepsilon\psi_t(\pi)-\varepsilon\psi_t(0)}{\int\limits_0^\pi xf(x,t,w)dx}$$

$$+\frac{\pi\sum\limits_{k=1}^{+\infty}\left(a_k\varphi'_{ck}\cos\alpha_k t+b_k\psi_{sk}\sin\alpha_k t+\frac{1}{\alpha_k}\int\limits_0^t s(\tau)f'_{ck}(\tau,w)\sin\alpha_k(t-\tau)d\tau\right)}{\int\limits_0^\pi xf(x,t,w)dx},$$

where $a_k=\frac{1}{1+4\varepsilon k^2}$, $b_k=\frac{1}{\sqrt{1+4\varepsilon k^2}}$. The iteration of the inverse coefficient of (3.1) is

$$s^{(N+1)}(t)=\frac{E''(t)+\varepsilon\psi_t(\pi)-\varepsilon\psi_t(0)}{\int\limits_0^\pi xf(x,t,w^{(N)})dx}$$
$$-\frac{\pi\sum\limits_{k=1}^{+\infty}\left(a_k\varphi'_{ck}\cos\alpha_k t+b_k\psi_{sk}\sin\alpha_k t+\frac{1}{\alpha_k}\int\limits_0^t s^{(N)}(\tau)f'_{ck}(\tau,w^{(N)})\sin\alpha_k(t-\tau)d\tau\right)}{\int\limits_0^\pi xf(x,t,w^{(N)})dx}.$$

For $N=0$, we have

$$s^{(1)}(t)=\frac{E''(t)+\varepsilon\psi_t(\pi)-\varepsilon\psi_t(0)}{\int\limits_0^\pi xf(x,t,w^{(0)})dx}$$
$$-\frac{\pi\sum\limits_{k=1}^{+\infty}\left(a_k\varphi'_{ck}\cos\alpha_k t+b_k\psi_{sk}\sin\alpha_k t+\frac{1}{\alpha_k}\int\limits_0^t s^{(0)}(\tau)f'_{ck}(\tau,w^{(0)})\sin\alpha_k(t-\tau)d\tau\right)}{\int\limits_0^\pi xf(x,t,w^{(0)})dx}.$$

By adding and subtracting the integral $\int\limits_0^t\int\limits_0^\pi s^{(0)}(\tau)f(\xi,\tau,0)d\xi d\tau$ to the right-hand side of the equation, taking the absolute value, and subsequently applying the Cauchy inequality, we obtain

$$\left|s^{(1)}(t)\right|\le\frac{2}{\pi^2M}\left(\pi\sum_{k=1}^{+\infty}\left(|a_k\varphi'_{ck}|+|b_k\psi'_{ck}|\right)+|\varepsilon\psi_t(\pi)|+|\varepsilon\psi_t(0)|+|E''(t)|\right)$$
$$+\frac{2}{\pi M}\sum_{k=1}^{+\infty}\frac{1}{\alpha_k}\left(\int\limits_0^t d\tau\right)^{\frac12}\left(\int\limits_0^t\left(\frac{2}{\pi}\int\limits_0^\pi s^{(0)}(\tau)f'(\xi,\tau,0)\cos2k\xi\sin\alpha_k(t-\tau)d\xi\right)^2d\tau\right)^{\frac12}$$
$$+\frac{2}{\pi M}\sum_{k=1}^{+\infty}\frac{1}{\alpha_k}\left(\int\limits_0^t d\tau\right)^{\frac12}$$
$$\times\left(\int\limits_0^t\left(\frac{2}{\pi}\int\limits_0^\pi s^{(0)}(\tau)[f'(\xi,\tau,w^{(0)})-f'(\xi,\tau,0)]\cos2k\xi\sin\alpha_k(t-\tau)d\xi\right)^2d\tau\right)^{\frac12},$$

where $\left|\int\limits_0^\pi xf(x,t,w^{(0)})dx\right|\le\frac{\pi^2M}{2}$. By successively applying Hölder's and Bessel's inequalities, imposing the Lipschitz condition, and taking the maximum over $t\in[0,T]$,

we obtain

$$\begin{aligned}\left\|s^{(1)}(t,\varepsilon)\right\| \leq & \frac{2}{\pi^2 M}\left(\|E''(t,\varepsilon)\|+\|\varepsilon\psi_t(\pi)\|+\|\varepsilon\psi_t(0)\|+\pi\mu\sum_{k=1}^{+\infty}\|\varphi'_{ck}\|+\pi\eta\sum_{k=1}^{+\infty}\|\psi_{sk}\|\right)\\ &+\frac{4\,|T|}{M}\left\|s^{(0)}(t)\right\|\cdot\|b(x,t)\|\cdot\left\|w^{(0)}(t,\varepsilon)\right\|\sqrt{\frac{T}{\pi}\left(\frac{\pi^2}{24}+\varepsilon\right)}\\ &+4\,|T|\cdot\left\|s^{(0)}(t)\right\|\sqrt{\frac{T}{\pi}\left(\frac{\pi^2}{24}+\varepsilon\right)},\end{aligned}$$

where $\left(\sum\limits_{k=1}^{+\infty}|a_k|^2\right)^{\frac{1}{2}}=\mu$, $\left(\sum\limits_{k=1}^{+\infty}|b_k|^2\right)^{\frac{1}{2}}=\eta$, $\left(\sum\limits_{k=1}^{+\infty}\frac{1}{\alpha_k^2}\right)^{\frac{1}{2}}=\sqrt{\frac{\pi^2}{24}+\varepsilon}$. The estimations for the subsequent step $N+1$:

$$\begin{aligned}\left\|w^{(N+1)}(t,\varepsilon)\right\| \leq & \frac{\|\varphi_0\|+\|\psi_0\|\cdot|T|}{2}+\sum_{k=1}^{+\infty}\left(\|\varphi_{ck}\|+\|\varphi_{sk}\|\right)+\sum_{k=1}^{+\infty}\left(\|\psi_{ck}\|+\|\psi_{sk}\|\right)\sqrt{\frac{\pi^2}{24}+\varepsilon}\\ &+\left(T^2\sqrt{\frac{\pi T}{3}}+4T\sqrt{\pi T\left(\frac{\pi^2}{24}+\varepsilon\right)}\right)\left\|s^{(N)}(t)\right\|\cdot\|b(x,t)\|\cdot\left\|w^{(N)}(t,\varepsilon)\right\|\\ &+\left(T^2\sqrt{\frac{\pi T}{3}}+4T\sqrt{\pi T\left(\frac{\pi^2}{24}+\varepsilon\right)}\right)\left\|s^{(N)}(t)\right\|\cdot\|f(x,t,0)\|,\\ \left\|s^{(N+1)}(t,\varepsilon)\right\| \leq & \frac{2}{\pi^2 M}\left(\|E''(t,\varepsilon)\|+\|\varepsilon\psi_t(\pi)\|+\|\varepsilon\psi_t(0)\|+\pi\mu\sum_{k=1}^{+\infty}\|\varphi'_{ck}\|+\pi\eta\sum_{k=1}^{+\infty}\|\psi_{sk}\|\right)\\ &+\frac{4\,|T|}{M}\left\|s^{(N)}(t)\right\|\cdot\|b(x,t)\|\cdot\left\|w^{(N)}(t,\varepsilon)\right\|\sqrt{\frac{T}{\pi}\left(\frac{\pi^2}{24}+\varepsilon\right)}\\ &+4\,|T|\left\|s^{(N)}(t)\right\|\sqrt{\frac{T}{\pi}\left(\frac{\pi^2}{24}+\varepsilon\right)}.\end{aligned}$$

From $w^{(N)}(t)\in B$, $t\in[0,T]$ and the theorem, we obtain $w^{(N+1)}(t)\in B$, $t\in[0,T]$.

To establish $\lim\limits_{N\to+\infty}w^{(N+1)}(t,\varepsilon)=w^{(N)}(t,\varepsilon)$, $\lim\limits_{N\to+\infty}s^{(N+1)}(t)=s^{(N)}(t)$, let us first take the difference of

$$\begin{aligned}w_0^{(1)}(t)-w_0^{(0)}(t)&=\frac{2}{\pi}\int_0^t\int_0^\pi s^{(0)}(\tau)(t-\tau)f(\xi,\tau,w^{(0)})d\xi d\tau,\\ w_{ck}^{(1)}(t)-w_{ck}^{(0)}(t)&=\frac{1}{\alpha_k}\cdot\frac{2}{\pi}\int_0^t\int_0^\pi s^{(0)}(\tau)f(\xi,\tau,w^{(0)})\cos 2k\xi\sin\alpha_k(t-\tau)d\xi d\tau,\\ w_{sk}^{(1)}(t)-w_{sk}^{(0)}(t)&=\frac{1}{\alpha_k}\cdot\frac{2}{\pi}\int_0^t\int_0^\pi s^{(0)}(\tau)f(\xi,\tau,w^{(0)})\sin 2k\xi\sin\alpha_k(t-\tau)d\xi d\tau.\end{aligned}$$

By adding and subtracting the term $\int_0^t \int_0^\pi s^{(0)}(\tau) f(\xi,\tau,0) d\xi d\tau$ on the right-hand sides of the equations, and successively applying Cauchy, Bessel, and Hölder inequalities followed by the Lipschitz condition, we obtain the following estimate by taking the maximum over $t \in [0,T]$:

$$\begin{aligned}\left\|w^{(1)}(t)-w^{(0)}(t)\right\| \leq & \left(T^2\sqrt{\frac{\pi T}{3}}+4T\sqrt{\frac{T\pi^3}{24}+\pi T\varepsilon}\right)\|f(\xi,\tau,0)\|\cdot\left\|s^{(0)}(t)\right\| \\ & +\left(T^2\sqrt{\frac{\pi T}{3}}+4T\sqrt{\frac{T\pi^3}{24}+\pi T\varepsilon}\right)\|b(x,t)\|\cdot\left\|s^{(0)}(t)\right\|\cdot\left\|w^{(0)}(t)\right\|.\end{aligned}$$

Let

$$K := \left\|w^{(1)}(t)-w^{(0)}(t)\right\| < +\infty. \tag{3.2}$$

If successive differences are taken for the inverse coefficient and the same methods are applied, we have

$$\left\|s^{(1)}(t)-s^{(0)}(t)\right\| \leq \frac{R}{1-RM}\left\|s^{(1)}(t)\right\|\cdot\|b(x,t)\|\cdot\left\|w^{(1)}(t)-w^{(0)}(t)\right\|, \tag{3.3}$$

where $R=\frac{4|T|}{M}\sqrt{\frac{T\pi}{24}+\frac{T\varepsilon}{\pi}}$, $M=\left\|f'(\xi,\tau,w^{(0)})\right\|$. Applying the same procedure to the subsequent difference yields

$$\begin{aligned}\left\|w^{(2)}(t)-w^{(1)}(t)\right\| \leq & \left(T^2\sqrt{\frac{\pi T}{3}}+4T\sqrt{\frac{T\pi^3}{24}+\pi T\varepsilon}\right)\|b(x,t)\|\cdot\left\|s^{(1)}(t)\right\| \\ & \times\left\|w^{(1)}(t)-w^{(0)}(t)\right\| \\ & +\left(T^2\sqrt{\frac{\pi T}{3}}+4T\sqrt{\frac{T\pi^3}{24}+\pi T\varepsilon}\right)\left\|s^{(1)}(t)-s^{(0)}(t)\right\| \\ & \times\left\|f(\xi,\tau,w^{(0)})\right\|.\end{aligned} \tag{3.4}$$

Substituting (3.2) and (3.3) into (3.4), we obtain

$$\left\|w^{(2)}(t)-w^{(1)}(t)\right\| \leq \left(\frac{A}{1-RM}\right)K\left\|s^{(1)}(t)\right\|\left(\int_0^t\int_0^\pi b^2(\xi,\tau)d\xi d\tau\right)^{\frac{1}{2}}, \tag{3.5}$$

where $A=T^2\sqrt{\frac{\pi T}{3}}+4T\sqrt{\frac{T\pi^3}{24}+\pi T\varepsilon}$. Applying the same method to the next difference, we obtain

$$\left\|s^{(2)}(t)-s^{(1)}(t)\right\| \leq \frac{R}{1-RM}\left\|s^{(2)}(t)\right\|\cdot\|b(x,t)\|\cdot\left\|w^{(2)}(t)-w^{(1)}(t)\right\|, \tag{3.6}$$

$$\begin{aligned}\left\|w^{(3)}(t)-w^{(2)}(t)\right\| \leq & A\|b(x,t)\|\cdot\left\|s^{(2)}(t)\right\|\cdot\left\|w^{(2)}(t)-w^{(1)}(t)\right\| \\ & +A\left\|s^{(2)}(t)-s^{(1)}(t)\right\|\cdot\left\|f(\xi,\tau,w^{(0)})\right\|.\end{aligned} \tag{3.7}$$

Substituting (3.5) and (3.6) into (3.7), we obtain

$$\left\|w^{(3)}(t)-w^{(2)}(t)\right\| \leq \left(\frac{A}{1-RM}\right)^2 K \left\|s^{(1)}(t)\right\| \cdot \left\|s^{(2)}(t)\right\| \times \left(\int_0^t \int_0^\pi b^2(\xi,\tau)\left(\int_0^t \int_0^\pi b^2(\tilde{\xi},\tilde{\tau})d\tilde{\xi}d\tilde{\tau}\right)^{\frac{1}{2}} d\xi d\tau\right)^{\frac{1}{2}}.$$

If the method of change of variables is applied to the integral, we obtain

$$\left\|w^{(3)}(t)-w^{(2)}(t)\right\| \leq \left(\frac{A}{1-RM}\right)^2 K \left\|s^{(1)}(t)\right\| \cdot \left\|s^{(2)}(t)\right\| \frac{1}{\sqrt{2}}\left(\left(\int_0^t \int_0^\pi b^2(\xi,\tau)d\xi d\tau\right)^2\right)^{\frac{1}{2}}.$$

If the same method is applied up to the $(N+1)$th iteration, we have

(3.8)

$$\left\|w^{(N+1)}(t)-w^{(N+1)}(t)\right\| \leq \left(\frac{A}{1-RM}\right)^N K \prod_{i=1}^N \left\|s^{(i)}(t)\right\| \frac{1}{\sqrt{N!}}\left(\left(\int_0^t \int_0^\pi b^2(\xi,\tau)d\xi d\tau\right)^N\right)^{\frac{1}{2}}$$

and

$$\left\|s^{(N+1)}(t)-s^{(N)}(t)\right\| \leq \frac{R}{1-RM}\left\|s^{(N)}(t)\right\| \cdot \|b(x,t)\| \cdot \left\|w^{(N+1)}(t)-w^{(N)}(t)\right\|. \tag{3.9}$$

We deduce that $w^{(N+1)} \to w^{(N)}$ when $N \to +\infty$, hence $s^{(N+1)} \to s^{(N)}$. Let us show that $\lim\limits_{N\to+\infty} w^{(N+1)}(t,\varepsilon) = w(t,\varepsilon)$, $\lim\limits_{N\to+\infty} s^{(N+1)}(t) = s(t)$.

We consider the following difference for the inverse coefficient:

$$s(t)-s^{(N+1)}(t) = \frac{-\pi \sum\limits_{k=1}^{+\infty} \frac{1}{\alpha_k} \cdot \frac{2}{\pi} \int\limits_0^t \int\limits_0^\pi s(\tau) f'(\xi,\tau,w)\cos 2k\xi \sin\alpha_k(t-\tau)d\xi d\tau}{\int\limits_0^\pi x f(\xi,\tau,w)dx} + \frac{\pi \sum\limits_{k=1}^{+\infty} \frac{1}{\alpha_k} \cdot \frac{2}{\pi} \int\limits_0^t \int\limits_0^\pi s^{(N+1)}(\tau) f'(\xi,\tau,w^{(N+1)})\cos 2k\xi \sin\alpha_k(t-\tau)d\xi d\tau}{\int\limits_0^\pi x f(\xi,\tau,w^{(N+1)})dx}.$$

By adding and subtracting the term $\int\limits_0^t \int\limits_0^\pi s(\tau) f(\xi,\tau,w^{(N+1)})d\xi d\tau$ and taking absolute value, we have

$$\left|s(t)-s^{(N+1)}(t)\right| \leq \frac{2\sum\limits_{k=1}^{+\infty}\left|\frac{1}{\alpha_k}\cdot\frac{2}{\pi}\int\limits_0^t\int\limits_0^\pi \left[s(\tau)-s^{(N+1)}(\tau)\right] f'(\xi,\tau,w^{(N+1)})\cos 2k\xi\sin\alpha_k(t-\tau)d\xi d\tau\right|}{\pi M} + \frac{2\sum\limits_{k=1}^{+\infty}\left|\frac{1}{\alpha_k}\cdot\frac{2}{\pi}\int\limits_0^t\int\limits_0^\pi s(\tau)\left[f'(\xi,\tau,w)-f'(\xi,\tau,w^{(N+1)})\right]\cos 2k\xi\sin\alpha_k(t-\tau)d\xi d\tau\right|}{\pi M},$$

where $\left|\int_0^\pi xf(\xi,\tau,w)dx\right| \le \frac{\pi^2 M}{2}$, $\left|\int_0^\pi xf(\xi,\tau,w^{(N+1)})dx\right| \le \frac{\pi^2 M}{2}$. By successively applying the Cauchy, Hölder, and Bessel's inequalities along with the Lipschitz condition to the obtained inequality, and taking the maximum over $t \in [0,T]$, we obtain

$$\left\|s(t)-s^{(N+1)}(t)\right\| \le \frac{R\left\|s(t)\right\|\cdot\left\|b(x,t)\right\|}{1-RM}\left\|w(t)-w^{(N+1)}(t)\right\|, \tag{3.10}$$

where $R=\frac{4|T|}{M}\sqrt{\frac{T\pi}{24}+\frac{T\varepsilon}{\pi}}$, $M=\left\|f(x,t,w^{(N+1)})\right\|$. By taking the difference between the exact solution and the sequential solution, we have

$$\begin{aligned}
w_0(t)-w_0^{(N+1)}(t) =& \frac{2}{\pi}\int_0^t\int_0^\pi (t-\tau)s(\tau)f(\xi,\tau,w)d\xi d\tau \\
&-\frac{2}{\pi}\int_0^t\int_0^\pi (t-\tau)s^{(N)}(\tau)f(\xi,\tau,w^{(N)})d\xi d\tau,\\
w_{ck}(t)-w_{ck}^{(N+1)}(t) =& \sum_{k=1}^{+\infty}\frac{1}{\alpha_k}\cdot\frac{2}{\pi}\int_0^t\int_0^\pi s(\tau)f(\xi,\tau,w)\cos 2k\xi\sin\alpha_k(t-\tau)d\xi d\tau \\
&-\sum_{k=1}^{+\infty}\frac{1}{\alpha_k}\cdot\frac{2}{\pi}\int_0^t\int_0^\pi s^{(N)}(\tau)f(\xi,\tau,w^{(N)})\cos 2k\xi\sin\alpha_k(t-\tau)d\xi d\tau,\\
w_{sk}(t)-w_{sk}^{(N+1)}(t) =& \sum_{k=1}^{+\infty}\frac{1}{\alpha_k}\cdot\frac{2}{\pi}\int_0^t\int_0^\pi s(\tau)f(\xi,\tau,w)\sin 2k\xi\sin\alpha_k(t-\tau)d\xi d\tau \\
&-\sum_{k=1}^{+\infty}\frac{1}{\alpha_k}\cdot\frac{2}{\pi}\int_0^t\int_0^\pi s^{(N)}(\tau)f(\xi,\tau,w^{(N)})\sin 2k\xi\sin\alpha_k(t-\tau)d\xi d\tau.
\end{aligned}$$

By adding and subtracting the term

$$\int_0^t\int_0^\pi s(\tau)f(\xi,\tau,w^{(N)})d\xi d\tau, \quad \int_0^t\int_0^\pi s(\tau)f(\xi,\tau,w^{(N+1)})d\xi d\tau$$

and $\int_0^t\int_0^\pi s^{(N+1)}(\tau)f(\xi,\tau,w^{(N)})d\xi d\tau$ on the right-hand sides of the equations, and successively applying Cauchy, Bessel, and Hölder inequalities followed by the Lipschitz condition, we obtain the following estimate by taking the maximum over $t\in[0,T]$:

$$\begin{aligned}
\left\|w(t)-w^{(N+1)}(t)\right\| \le& \left(T^2\sqrt{\frac{\pi T}{3}}+4T\sqrt{\pi T\left(\frac{\pi^2}{24}+\varepsilon\right)}\right)\left\|s(t)\right\| \\
&\times\left\|b(x,t)\right\|\cdot\left\|w(t)-w^{(N+1)}(t)\right\| \\
&+\left(T^2\sqrt{\frac{\pi T}{3}}+4T\sqrt{\pi T\left(\frac{\pi^2}{24}+\varepsilon\right)}\right)\left\|s^{(N+1)}(t)-s^{(N)}(t)\right\|
\end{aligned} \tag{3.11}$$

$$\times \left\| f(x,t,w^{(N)}) \right\| + \left(T^2\sqrt{\frac{\pi T}{3}} + 4T\sqrt{\pi T\left(\frac{\pi^2}{24}+\varepsilon\right)} \right) \left\| s(t) - s^{(N+1)}(t) \right\| \times \left\| f(x,t,w^{(N)}) \right\| + \left(T^2\sqrt{\frac{\pi T}{3}} + 4T\sqrt{\pi T\left(\frac{\pi^2}{24}+\varepsilon\right)} \right) \|s(t)\| \cdot \|b(x,t)\| \times \left\| w^{(N+1)}(t) - w^{(N)}(t) \right\|.$$

Substituting (3.8)–(3.10) into (3.11), we obtain

$$\left\| w(t) - w^{(N+1)}(t) \right\| \le \left(\frac{A}{1-RM} \right) \|b(x,t)\| \cdot \|s(t)\| \cdot \left\| w(t) - w^{(N+1)}(t) \right\| + \left(\frac{ARM}{1-RM} \left\| s^{(N+1)}(t) \right\| + A\|s(t)\| \right) \left(\frac{A}{1-RM} \right)^N K \times \prod_{i=1}^{N} \left\| s^{(i)}(t) \right\| \frac{\|b(x,t)\|^{N+1}}{\sqrt{(N+1)!}}.$$

By applying $(a+b)^2 \le 2a^2 + 2b^2$ inequality, we obtain

$$\left\| w(t) - w^{(N+1)}(t) \right\|^2 \le 2\left(\frac{A}{1-RM} \right)^2 \left(\int_0^t \int_0^\pi \left(s(\tau) b(\xi,\tau) \left| w(\tau) - w^{(N+1)}(\tau) \right| \right)^2 d\xi d\tau \right) + 2\left(\left(\frac{ARM}{1-RM} \left\| s^{(N+1)}(t) \right\| + A\|s(t)\| \right) \left(\frac{A}{1-RM} \right)^N K \times \prod_{i=1}^{N} \left\| s^{(i)}(t) \right\| \frac{\|b(x,t)\|^{N+1}}{\sqrt{(N+1)!}} \right)^2.$$

Applying Gronwall's inequality, we obtain

$$\left\| \nu(\psi) - \nu^{(N+1)}(\psi) \right\|^2 \le 2Ae^{2\left(\frac{A}{1-RM}\right)^2 \left(\int_0^t \int_0^\pi (s(\tau)b(\xi,\tau))^2 d\xi d\tau \right)} \left(\frac{RM}{1-RM} \left\| s^{(N+1)}(t) \right\| + \|s(t)\| \right)^2 \times \left(\left(\frac{A}{1-RM} \right)^N K \prod_{i=1}^{N} \left\| s^{(i)}(t) \right\| \frac{\|b(x,t)\|^{N+1}}{\sqrt{(N+1)!}} \right)^2.$$

That is, $w^{(N+1)} \to w$, $s^{(N+1)} \to s$, when $N \to +\infty$.

Let (w,s) and (v,q) be two solutions of (2.1)–(2.4). We consider the difference between the corresponding inverse coefficients:

$$s(t) - q(t) = \frac{-\pi \sum_{k=1}^{+\infty} \frac{1}{\alpha_k} \cdot \frac{2}{\pi} \int_0^t \int_0^\pi s(\tau) f'(\xi,\tau,w) \cos 2k\xi \sin \alpha_k (t-\tau) d\xi d\tau}{\int_0^\pi x f(x,t,w) dx}$$

$$- \frac{-\pi \sum\limits_{k=1}^{+\infty} \frac{1}{\alpha_k} \cdot \frac{2}{\pi} \int\limits_0^t \int\limits_0^\pi q(\tau) f'(\xi,\tau,\nu) \cos 2k\xi \sin \alpha_k (t-\tau) d\xi d\tau}{\int\limits_0^\pi x f(x,t,\nu) dx}.$$

By adding and subtracting the term $\int\limits_0^t \int\limits_0^\pi s(\tau) f'(\xi,\tau,\nu) d\xi d\tau$ on the right-hand side of the equation, and successively applying Cauchy, Bessel, and Hölder inequalities followed by the Lipschitz condition, we obtain the following estimate by taking the maximum over $t \in [0,T]$:

$$\|s(t) - q(t)\| \leq \frac{R}{1 - RM} \|b(x,t)\| \cdot \|s(t)\| \cdot \|w(t) - \nu(t)\|, \tag{3.12}$$

where $R = \frac{4|T|}{M} \sqrt{\frac{T\pi}{24} + \frac{T\varepsilon}{\pi}}$, $M = \|f'(x,t,\nu)\|$. Taking the difference between the two solutions, we have

$$\begin{aligned}
w_0(t) - \nu_0(t) =& \frac{2}{\pi} \int\limits_0^t \int\limits_0^\pi f(\xi,\tau,w)(t-\tau) s(\tau) d\xi d\tau - \frac{2}{\pi} \int\limits_0^t \int\limits_0^\pi f(\xi,\tau,\nu)(t-\tau) q(\tau) d\xi d\tau, \\
w_{ck}(t) - \nu_{ck}(t) =& \sum_{k=1}^{+\infty} \frac{1}{\alpha_k} \cdot \frac{2}{\pi} \int\limits_0^t \int\limits_0^\pi s(\tau) f(\xi,\tau,w) \cos 2k\xi \sin \alpha_k (t-\tau) d\xi d\tau \\
&+ \sum_{k=1}^{+\infty} \frac{1}{\alpha_k} \cdot \frac{2}{\pi} \int\limits_0^t \int\limits_0^\pi q(\tau) f(\xi,\tau,\nu) \cos 2k\xi \sin \alpha_k (t-\tau) d\xi d\tau, \\
w_{sk}(t) - \nu_{sk}(t) =& \sum_{k=1}^{+\infty} \frac{1}{\alpha_k} \cdot \frac{2}{\pi} \int\limits_0^t \int\limits_0^\pi s(\tau) f(\xi,\tau,w) \sin 2k\xi \sin \alpha_k (t-\tau) d\xi d\tau \\
&- \sum_{k=1}^{+\infty} \frac{1}{\alpha_k} \cdot \frac{2}{\pi} \int\limits_0^t \int\limits_0^\pi q(\tau) f(\xi,\tau,\nu) \sin 2k\xi \sin \alpha_k (t-\tau) d\xi d\tau.
\end{aligned}$$

Applying the same methods as above, we obtain

$$\begin{aligned}
\|w(t) - \nu(t)\| \leq& \left(T^2 \sqrt{\frac{\pi T}{3}} + 4|T| \sqrt{\pi T \left(\frac{\pi^2}{24} + \varepsilon \right)} \right) \|s(t)\| \cdot \|b(x,t)\| \cdot \|w(t) - \nu(t)\| \\
&+ \left(T^2 \sqrt{\frac{\pi T}{3}} + 4|T| \sqrt{\pi T \left(\frac{\pi^2}{24} + \varepsilon \right)} \right) \|s(t) - q(t)\| \cdot \|f(x,t,\nu)\|
\end{aligned} \tag{3.13}$$

Substituting (3.12) into (3.13), we obtain

$$\|w(t) - \nu(t)\| \leq \left(\frac{A}{1 - RM} \right) \left(\int\limits_0^t \int\limits_0^\pi \left(s(\tau) b(\xi,\tau) |w(\tau) - \nu(\tau)| \right)^2 d\xi d\tau \right)^{\frac{1}{2}},$$

where $A = T^2\sqrt{\frac{\pi T}{3}} + 4\,|T|\,\sqrt{\pi T\left(\frac{\pi^2}{24}+\varepsilon\right)}$.

By squaring the obtained inequality and applying the Gronwall inequality, we obtain

$$\|w(t)-\nu(t)\|^2 \le 0\cdot e^{\left(\frac{A}{1-RM}\right)^2}\int\limits_0^t\int\limits_0^\pi (s(\tau)b(\xi,\tau))^2 d\xi d\tau.$$

As a result $w(t)=v(t)$, therefore $s(t)=q(t)$. The proof is completed. □

4. Stability of the Solution

Theorem 4.1. *Let assumptions* (A1)-(A3) *be satisfied. Then, the solution* (w,s) *of problem* (2.1)–(2.4) *depends continuously on the input data* ϕ, ψ *and* E.

Proof. Consider two sets of data

$$\Phi=(\varphi,\psi,E), \quad \bar{\Phi}=\left(\bar{\varphi},\bar{\psi},\bar{E}\right)$$

both satisfying the assumptions of Theorem 3.1. Assume that there exist positive constants M_1, M_2, M_3 such that

$$\|E\|_{C^2[0,T]}\le M_1, \quad \|\varphi\|_{C^1[0,T]}\le M_2, \quad \|\psi\|_{C^1[0,T]}\le M_3,$$

and similarly

$$\left\|\bar{E}\right\|_{C^2[0,T]}\le M_1, \quad \|\bar{\varphi}\|_{C^1[0,T]}\le M_2, \quad \left\|\bar{\psi}\right\|_{C^1[0,T]}\le M_3.$$

Define the norms

$$\|\Phi\|=\|\varphi\|_{C^1[0,T]}+\|\psi\|_{C^1[0,T]}+\|E\|_{C^2[0,T]}, \quad \left\|\bar{\Phi}\right\|=\|\bar{\varphi}\|_{C^1[0,T]}+\left\|\bar{\psi}\right\|_{C^1[0,T]}+\left\|\bar{E}\right\|_{C^2[0,T]}.$$

Let the solutions (w,s) and $(\bar{w},\bar{s})$ correspond to data Φ and $\bar{\Phi}$, respectively. First, the inverse coefficient

$$s(t)=\int\limits_0^t \Upsilon(t,\tau)s(\tau)d\tau+\Phi(t)$$

will be examined, where

$$\Phi(t)=\frac{E''(t)+\varepsilon\psi_t(\pi)-\varepsilon\psi_t(0)}{\int\limits_0^\pi xf(x,t,w)dx} + \frac{\pi\sum\limits_{k=1}^{+\infty}(2k)\left(\left(\varepsilon\alpha_k^2-1\right)\varphi_{sk}\cos\alpha_k t+\left(\varepsilon\alpha_k-\frac{1}{\alpha_k}\right)\psi_{sk}\sin\alpha_k t\right)}{\int\limits_0^\pi xf(x,t,w)dx},$$

$$\Upsilon(t,\tau)=\frac{-\pi\sum\limits_{k=1}^{+\infty}\frac{2k}{\alpha_k}f_{sk}(\tau)\sin\alpha_k(t-\tau)}{\int\limits_0^\pi xf(x,t,w)dx}.$$

For the difference of the inverse coefficients, adding and subtracting $\bar{s}(t)\Upsilon(t,\tau)$ yields

$$s(t)-\bar{s}(t)=\int_0^t s(\tau)\Upsilon(t,\tau)d\tau-\int_0^t \bar{s}(\tau)\bar{\Upsilon}(t,\tau)d\tau+\Phi(t)-\bar{\Phi}(t).$$

Taking the maximum, we obtain

$$\|s(t)-\bar{s}(t)\|\le\frac{1}{1-|T|\cdot\|\Upsilon\|}\left\|\Phi-\bar{\Phi}\right\|+\frac{|T|\cdot\|\bar{s}(\tau)\|}{1-|T|\cdot\|\Upsilon\|}\left\|\Upsilon-\bar{\Upsilon}\right\|, \tag{4.1}$$

where $|T|\cdot\|\Upsilon\|\le 1$,

$$\Phi-\bar{\Phi}=\frac{E''(t)+\varepsilon\psi_t(\pi)-\varepsilon\psi_t(0)+\pi\sum\limits_{k=1}^{+\infty}\left(a_k\varphi'_{ck}\cos\alpha_k t+b_k\psi'_{ck}\sin\alpha_k t\right)}{\int\limits_0^\pi xf(x,t,w)dx}$$
$$-\frac{\bar{E}''(t)+\varepsilon\bar{\psi}_t(\pi)-\varepsilon\bar{\psi}_t(0)+\pi\sum\limits_{k=1}^{+\infty}\left(a_k\bar{\varphi}'_{ck}\cos\alpha_k t+b_k\bar{\psi}'_{ck}\sin\alpha_k t\right)}{\int\limits_0^\pi xf(x,t,\bar{w})dx}.$$

Here $a_k=\varepsilon\alpha_k^2-1$, $b_k=\varepsilon\alpha_k-\frac{1}{\alpha_k}$. By adding and subtracting $E''(t)\int\limits_0^\pi xf(x,t,w)dx$,

$$\varphi'_{ck}\cos 2kt\int_0^\pi xf(x,t,w)dx,\quad \psi_{sk}\sin 2kt\int_0^\pi xf(x,t,w)dx,\quad \varepsilon\psi_t(0)\int_0^\pi xf(x,t,w)dx$$

and $\varepsilon\psi_t(\pi)\int\limits_0^\pi xf(x,t,w)dx$ to the last equation, we have

$$\Phi-\bar{\Phi}=\frac{-E''(t)\int\limits_0^\pi x\left[f(x,t,w)-f(x,t,\bar{w})\right]dx+\left[E''(t)-\bar{E}''(t)\right]\int\limits_0^\pi xf(x,t,w)dx}{\int\limits_0^\pi xf(x,t,w)dx\int\limits_0^\pi xf(x,t,\bar{w})dx}$$
$$+\frac{-\varepsilon\psi_t(\pi)\int\limits_0^\pi x\left[f(x,t,w)-f(x,t,\bar{w})\right]dx-\varepsilon\left[\psi_t(\pi)-\bar{\psi}_t(\pi)\right]\int\limits_0^\pi xf(x,t,w)dx}{\int\limits_0^\pi xf(x,t,w)dx\int\limits_0^\pi xf(x,t,\bar{w})dx}$$
$$+\frac{-\varepsilon\psi_t(0)\int\limits_0^\pi x\left[f(x,t,w)-f(x,t,\bar{w})\right]dx+\varepsilon\left[\psi_t(0)-\bar{\psi}_t(0)\right]\int\limits_0^\pi xf(x,t,w)dx}{\int\limits_0^\pi xf(x,t,w)dx\int\limits_0^\pi xf(x,t,\bar{w})dx}$$
$$+\frac{-\pi\sum\limits_{k=1}^{+\infty}a_k\varphi'_{ck}\cos\alpha_k t\int\limits_0^\pi x\left[f(x,t,w)-f(x,t,\bar{w})\right]dx}{\int\limits_0^\pi xf(x,t,w)dx\int\limits_0^\pi xf(x,t,\bar{w})dx}$$

$$+\frac{\pi\sum\limits_{k=1}^{+\infty}a_k\left[\varphi'_{ck}-\bar{\varphi}'_{ck}\right]\cos\alpha_k t\int\limits_0^\pi xf(x,t,w)dx}{\int\limits_0^\pi xf(x,t,w)dx\int\limits_0^\pi xf(x,t,\bar{w})dx}$$

$$+\frac{-\pi\sum\limits_{k=1}^{+\infty}b_k\psi'_{ck}\sin\alpha_k t\int\limits_0^\pi x\left[f(x,t,w)-f(x,t,\bar{w})\right]dx}{\int\limits_0^\pi xf(x,t,w)dx\int\limits_0^\pi xf(x,t,\bar{w})dx}$$

$$+\frac{\pi\sum\limits_{k=1}^{+\infty}b_k\left[\psi'_{ck}-\bar{\psi}'_{ck}\right]\sin\alpha_k t\int\limits_0^\pi xf(x,t,w)dx}{\int\limits_0^\pi xf(x,t,w)dx\int\limits_0^\pi xf(x,t,\bar{w})dx}.$$

Taking the absolute value, applying the Cauchy and Hölder inequalities together with the Lipschitz condition, and taking the maximum, we obtain

$$\begin{aligned}\left\|\Phi-\bar{\Phi}\right\|\leq&\frac{4}{\pi^4M^2}\sqrt{\frac{\pi^3}{3}}\left(M\left\|E''(t)-\bar{E}''(t)\right\|+\varepsilon\left\|\psi_t(\pi)-\bar{\psi}_t(\pi)\right\|+\varepsilon\left\|\psi_t(0)-\bar{\psi}_t(0)\right\|\right)\\&+\frac{4\mu}{\pi^3M}\sqrt{\frac{\pi^3}{3}}\sum_{k=1}^{+\infty}\left\|\varphi'_{ck}-\bar{\varphi}'_{ck}\right\|+\frac{4\eta}{\pi^3M}\sqrt{\frac{\pi^3}{3}}\sum_{k=1}^{+\infty}\left\|\psi'_{ck}-\bar{\psi}'_{ck}\right\|\\&+\frac{4}{\pi^4M^2}\sqrt{\frac{\pi^3}{3}}\left(2\varepsilon M_2+M_3+\pi\left(\mu M_1+\eta M_2\right)\right)\|b(x,t)\|\cdot\|w(t)-\bar{w}(t)\|,\end{aligned}\tag{4.2}$$

$$\begin{aligned}\Upsilon-\bar{\Upsilon}=&\frac{-\pi\sum\limits_{k=1}^{+\infty}\frac{2}{\pi\alpha_k}\sin\alpha_k(t-\tau)\int\limits_0^\pi f'(x,t,w)\cos 2kxdx}{\int\limits_0^\pi xf(x,t,w)dx}\\&-\frac{-\pi\sum\limits_{k=1}^{+\infty}\frac{2}{\pi\alpha_k}\sin\alpha_k(t-\tau)\int\limits_0^\pi f'(x,t,\bar{w})\cos 2kxdx}{\int\limits_0^\pi xf(x,t,\bar{w})dx}.\end{aligned}$$

Adding and subtracting $\int\limits_0^\pi f'(x,t,w)\cos 2kxdx\int\limits_0^\pi xf(x,t,\bar{w})dx$ to the last equation, we obtain

$$\begin{aligned}\Upsilon-\bar{\Upsilon}=&\frac{2\sum\limits_{k=1}^{+\infty}\frac{1}{\alpha_k}\sin\alpha_k(t-\tau)\int\limits_0^\pi f'(x,t,w)\cos 2kxdx\int\limits_0^\pi x\left[f(x,t,w)-f(x,t,\bar{w})\right]dx}{\int\limits_0^\pi xf(x,t,w)dx\int\limits_0^\pi xf(x,t,\bar{w})dx}\\&-\frac{2\sum\limits_{k=1}^{+\infty}\frac{1}{\alpha_k}\sin\alpha_k(t-\tau)\int\limits_0^\pi\left[f'(x,t,w)-f'(x,t,\bar{w})\right]\cos 2kxdx\int\limits_0^\pi xf(x,\psi,w)dx}{\int\limits_0^\pi xf(x,t,w)dx\int\limits_0^\pi xf(x,t,\bar{w})dx}.\end{aligned}$$

Taking the absolute value, applying the Cauchy and Hölder, Bessel inequalities together with the Lipschitz condition, and taking the maximum, we obtain

$$\left\|\Upsilon-\bar{\Upsilon}\right\| \leq \frac{16}{\sqrt{3}\pi^2 M}\left\|b(x,t)\right\|\cdot\left\|w(t)-\bar{w}(t)\right\|\sqrt{\frac{\pi^2}{24}+\varepsilon}. \tag{4.3}$$

Substituting (4.2)–(4.3) into (4.1), we obtain

$$\begin{aligned}\left\|s(t)-\bar{s}(t)\right\| \leq & \frac{1}{1-|T|\cdot\|\Upsilon\|}\cdot\frac{4}{\pi^3M^2}\left(\sqrt{\frac{\pi}{3}}(2\varepsilon M_2+M_3+\pi\left(\mu M_1+\lambda M_2\right)\right. \\ & \left.+4\pi M\left|T\right|\cdot\|\bar{s}(t)\|\sqrt{\frac{\pi^2}{24}+\varepsilon}\right)\left\|b(x,t)\right\|\cdot\left\|w(t)-\bar{w}(t)\right\| \\ & +\frac{1}{1-|T|\cdot\|\Upsilon\|}\cdot\frac{4\sqrt{\pi}}{\sqrt{3}\pi^3M}\left(\left\|E''(t)-\bar{E}''(t)\right\|\right) \\ & +\frac{1}{1-|T|\cdot\|\Upsilon\|}\cdot\frac{4\sqrt{\pi}}{\sqrt{3}\pi^3M}\left(\pi\mu\sum_{k=1}^{+\infty}\left\|{\varphi'}_{ck}-{\bar{\varphi}'}_{ck}\right\|+\pi\eta\sum_{k=1}^{+\infty}\left\|{\psi'}_{ck}-{\bar{\psi}'}_{ck}\right\|\right) \\ & +\frac{1}{1-|T|\cdot\|\Upsilon\|}\cdot\frac{4\varepsilon\sqrt{\pi}}{\sqrt{3}\pi^3M^2}\left(\left\|\psi_t(\pi)-\bar{\psi}_t(\pi)\right\|+\left\|\psi_t(0)-\bar{\psi}_t(0)\right\|\right).\end{aligned} \tag{4.4}$$

Let us consider the difference between the solutions corresponding to the two data sets:

$$\begin{aligned}w(t)-\bar{w}(t)= & \frac{(\varphi_0-\bar{\varphi}_0)+\left(\psi_0-\bar{\psi}_0\right)t}{2} \\ & +\sum_{k=1}^{+\infty}\left((\varphi_{ck}-\bar{\varphi}_{ck})\cos\alpha_k t+\frac{\left(\psi_{ck}-\bar{\psi}_{ck}\right)}{\alpha_k}\sin\alpha_k t\right)\cos 2kx \\ & +\sum_{k=1}^{+\infty}\left((\varphi_{sk}-\bar{\varphi}_{sk})\cos\alpha_k t+\frac{\left(\psi_{sk}-\bar{\psi}_{sk}\right)}{\alpha_k}\sin\alpha_k t\right)\sin 2kx \\ & +\frac{1}{\pi}\int_0^t\int_0^\pi f(\xi,\tau,w)(t-\tau)s(\tau)d\xi d\tau-\frac{1}{\pi}\int_0^t\int_0^\pi f(\xi,\tau,\bar{w})(t-\tau)\bar{s}(\tau)d\xi d\tau \\ & +\sum_{k=1}^{+\infty}\left(\frac{1}{\alpha_k}\cdot\frac{2}{\pi}\int_0^t\int_0^\pi s(\tau)f(\xi,\tau,w)\cos 2k\xi\sin\alpha_k(t-\tau)d\xi d\tau\right)\cos 2kx \\ & -\sum_{k=1}^{+\infty}\left(\frac{1}{\alpha_k}\cdot\frac{2}{\pi}\int_0^t\int_0^\pi \bar{s}(\tau)f(\xi,\tau,\bar{w})\cos 2k\xi\sin\alpha_k(t-\tau)d\xi d\tau\right)\cos 2kx \\ & +\sum_{k=1}^{+\infty}\left(\frac{1}{\alpha_k}\cdot\frac{2}{\pi}\int_0^t\int_0^\pi s(\tau)f(\xi,\tau,w)\cos 2k\xi\sin\alpha_k(t-\tau)d\xi d\tau\right)\sin 2kx\end{aligned}$$

$$- \sum_{k=1}^{+\infty} \left(\frac{1}{\alpha_k} \cdot \frac{2}{\pi} \int_0^t \int_0^\pi \bar{s}(\tau) f(\xi, \tau, \bar{w}) \cos 2k\xi \sin \alpha_k (t-\tau) d\xi d\tau \right) \sin 2kx.$$

By adding and subtracting the term $\int_0^t \int_0^\pi s(\tau) f(\xi, \tau, \bar{w}) d\xi d\tau$ on the right-hand side of the equation, and successively applying Cauchy, Bessel, and Hölder inequalities followed by the Lipschitz condition, we obtain the following estimate by taking the maximum over $t \in [0, T]$:

$$\begin{aligned} \|w(t) - \bar{w}(t)\| \leq & \frac{\|\varphi_0 - \bar{\varphi}_0\|}{2} + \frac{\left\|\psi_0 - \bar{\psi}_0\right\| \cdot |T|}{2} + \sum_{k=1}^{+\infty} \left(\|\varphi_{ck} - \bar{\varphi}_{ck}\| + \|\varphi_{sk} - \bar{\varphi}_{sk}\| \right) \\ & + \sum_{k=1}^{+\infty} \left(\left\|\psi_{ck} - \bar{\psi}_{ck}\right\| + \left\|\psi_{sk} - \bar{\psi}_{sk}\right\| \right) \sqrt{\frac{\pi^2}{24} + \varepsilon} \\ & + \left(T^2 \sqrt{\frac{\pi T}{3}} + 4T \sqrt{\pi T \left(\frac{\pi^2}{24} + \varepsilon \right)} \right) \|b(x,t)\| \cdot \|s(t)\| \cdot \|w(t) - \bar{w}(t)\| \\ & + \left(T^2 \sqrt{\frac{\pi T}{3}} + 4T \sqrt{\pi T \left(\frac{\pi^2}{24} + \varepsilon \right)} \right) \|f(x,t,\bar{w})\| \cdot \|s(t) - \bar{s}(t)\|. \end{aligned} \tag{4.5}$$

Substituting (4.4) into (4.5), we obtain

$$\begin{aligned} \|w(t) - \bar{w}(t)\| \leq & \frac{\|\varphi_0 - \bar{\varphi}_0\|}{2} + \frac{\left\|\psi_0 - \bar{\psi}_0\right\| \cdot |T|}{2} + \sum_{k=1}^{+\infty} \left(\|\varphi_{ck} - \bar{\varphi}_{ck}\| + \|\varphi_{sk} - \bar{\varphi}_{sk}\| \right) \\ & + \sum_{k=1}^{+\infty} \left(\left\|\psi_{ck} - \bar{\psi}_{ck}\right\| + \left\|\psi_{sk} - \bar{\psi}_{sk}\right\| \right) \sqrt{\frac{\pi^2}{24} + \varepsilon} \\ & + \frac{4\sqrt{\pi} A}{\sqrt{3}\pi^3 \left(1 - |T| \cdot \|\Upsilon\|\right)} \left\| E''(t) - \bar{E}''(t) \right\| \\ & \frac{4\sqrt{\pi} A}{\sqrt{3}\pi^2 \left(1 - |T| \cdot \|\Upsilon\|\right)} \left(\mu \sum_{k=1}^{+\infty} \left\| \varphi'_{ck} - \bar{\varphi}'_{ck} \right\| + \eta \sum_{k=1}^{+\infty} \left\| \psi'_{ck} - \bar{\psi}'_{ck} \right\| \right) \\ & + \frac{4\varepsilon\sqrt{\pi} A}{\sqrt{3}\pi^3 M \left(1 - |T| \cdot \|\Upsilon\|\right)} \left(\left\|\psi_t(\pi) - \bar{\psi}_t(\pi)\right\| + \left\|\psi_t(0) - \bar{\psi}_t(0)\right\| \right) \\ & + \left(\frac{4\sqrt{\pi} A \left(2\varepsilon M_2 + M_3 + \pi \left(\mu M_1 + \eta M_2\right)\right)}{\sqrt{3}\pi^3 M \left(1 - |T| \cdot \|\Upsilon\|\right)} \right. \\ & \left. + \sqrt{\frac{\pi^2}{24} + \varepsilon} \frac{16A |T| \cdot \|\bar{s}(t)\|}{\pi^2 \left(1 - |T| \cdot \|\Upsilon\|\right)} + A \|s(t)\| \right) \\ & \times \left(\int_0^t \int_0^\pi \left(b(\xi, \tau) |w(\tau) - \bar{w}(\tau)| \right)^2 d\xi d\tau \right)^{\frac{1}{2}}, \end{aligned} \tag{4.6}$$

where $A = T^2\sqrt{\frac{\pi T}{3}} + 4T\sqrt{\pi T\left(\frac{\pi^2}{24}+\varepsilon\right)}$. Let

$$\begin{aligned}
\|\varphi-\bar{\varphi}\| =& \frac{\|\varphi_0-\bar{\varphi}_0\|}{2} + \sum_{k=1}^{+\infty}\left(\|\varphi_{ck}-\bar{\varphi}_{ck}\| + \|\varphi_{sk}-\bar{\varphi}_{sk}\|\right) \\
&+ \frac{4A\mu\sqrt{\pi}}{\sqrt{3}\pi^2\left(1-|T|\cdot\|\Upsilon\|\right)}\sum_{k=1}^{+\infty}\left\|\varphi'_{ck}-\bar{\varphi}'_{ck}\right\|, \\
\left\|\psi-\bar{\psi}\right\| =& \frac{\left\|\psi_0-\bar{\psi}_0\right\|\cdot|T|}{2} + \frac{4Ax\sqrt{\pi}}{\sqrt{3}\pi^2\left(1-\|\Upsilon\|\cdot|\Psi|\right)}\sum_{k=1}^{+\infty}\left\|\psi'_{ck}-\bar{\psi}'_{ck}\right\| \\
&+ \sqrt{\frac{\pi^2}{24}+\varepsilon}\sum_{k=1}^{+\infty}\left(\left\|\psi_{ck}-\bar{\psi}_{ck}\right\| + \left\|\psi_{sk}-\bar{\psi}_{sk}\right\|\right) \\
&+ \frac{4\varepsilon\sqrt{\pi}A\left(\left\|\psi_t(\pi)-\bar{\psi}_t(\pi)\right\| + \left\|\psi_t(0)-\bar{\psi}_t(0)\right\|\right)}{\sqrt{3}\pi^3 M\left(1-\|\Upsilon\|\cdot|T|\right)}.
\end{aligned}$$

By defining the constants M_4, M_5, M_6 and M_7 as follows:

$$\begin{aligned}
M_4 =& \max\left(\frac{1}{2}, 1, \frac{4A\mu\sqrt{\pi}}{\sqrt{3}\pi^2\left(1-|T|\cdot\|\Upsilon\|\right)}\right), \\
M_5 =& \max\left(\frac{|T|}{2}, \sqrt{\frac{\pi^2}{24}+\varepsilon}, \frac{4Ax\sqrt{\pi}}{\sqrt{3}\pi^2\left(1-|T|\cdot\|\Upsilon\|\right)}\right), \\
M_6 =& \frac{4\sqrt{\pi}A}{\sqrt{3}\pi^3\left(1-|T|\cdot\|\Upsilon\|\right)}, \\
M_7 =& \frac{4\sqrt{\pi}A\left(2\varepsilon M_2 + M_3 + \pi\left(\mu M_1 + \lambda M_2\right)\right)}{\sqrt{3}\pi^3 M\left(1-\|\Upsilon\|\cdot|T|\right)} \\
&+ \sqrt{\frac{\pi^2}{24}+\varepsilon}\frac{16A|T|\cdot\|\bar{s}(t)\|}{\pi^2\left(1-\|\Upsilon\|\cdot|T|\right)} + A\|s(t)\|.
\end{aligned}$$

It follows that (4.6) is formulated as:

$$\begin{aligned}
\|w(t)-\bar{w}(t)\| \leq& M_4\|\varphi-\bar{\varphi}\| + M_5\left\|\psi-\bar{\psi}\right\| + M_6\left\|E''(t)-\bar{E}''(t)\right\| \\
&+ M_7\left(\int_0^t\int_0^\pi\left(b(\xi,\tau)|w(\tau)-\bar{w}(\tau)|\right)^2 d\xi d\tau\right)^{\frac{1}{2}}.
\end{aligned}$$

Furthermore, by setting $M_8 = \max\{M_4, M_5, M_6\}$, the final inequality is derived as:

$$\|w(t)-\bar{w}(t)\| \leq M_8\left\|\Phi-\bar{\Phi}\right\| + M_7\left(\int_0^t\int_0^\pi\left(b(\xi,\tau)|w(\tau)-\bar{w}(\tau)|\right)^2 d\xi d\tau\right)^{\frac{1}{2}}.$$

Applying inequality $(a+b)^2 \leq 2a^2 + 2b^2$, we obtain

$$\|w(t) - \bar{w}(t)\|^2 \leq 2M_8^2 \left\|\Phi - \bar{\Phi}\right\|^2 + 2M_7^2 \int_0^t \int_0^\pi \left(b(\xi,\tau)\left|w(\tau) - \bar{w}(\tau)\right|\right)^2 d\xi d\tau.$$

Finally, by employing Gronwall's inequality, we obtain

$$\|w(t) - \bar{w}(t)\|^2 \leq 2M_8^2 \left\|\Phi - \bar{\Phi}\right\|^2 e^{2M_7^2 \int_0^t \int_0^\pi b(\xi,\tau) d\xi d\tau}.$$

When the functions Φ and Φ', which represent the input data, approach each other, it follows that $w \to \bar{w}$ and $s \to \bar{s}$. This demonstrates that the system is stable with respect to the initial conditions. □

5. The Numerical Procedure

We devise an iterative algorithm aimed at linearizing the problem,

$$\frac{\partial^2 w^{(n)}}{\partial t^2} = \varepsilon \frac{\partial^4 w^{(n)}}{\partial x^2 \partial t^2} + \frac{\partial^2 w^{(n)}}{\partial x^2} + s(t) f(x,t,w^{(n-1)}), \tag{5.1}$$

$$\begin{aligned} w^{(n)}(x,0) &= \varphi(x), \quad x \in [0,\pi], \\ w_t^{(n)}(x,0) &= \psi(x), \quad x \in [0,\pi], \\ w^{(n)}(0,t) &= w^{(n)}(\pi,t), \quad t \in [0,T], \end{aligned} \tag{5.2}$$

$$w_x^{(n)}(0,t) = w_x^{(n)}(\pi,t). \tag{5.3}$$

By setting $w^{(n)}(x,t) = v(x,t)$ and $f\left(x,t,w^{(n-1)}\right) = \tilde{f}(x,t)$, we can express the problem (5.1)–(5.3) as a linear problem

$$\frac{\partial^2 v}{\partial t^2} = \varepsilon \frac{\partial^4 v}{\partial x^2 \partial t^2} + \frac{\partial^2 v}{\partial x^2} + s(t)\tilde{f}(x,t), \quad (x,t) \in D. \tag{5.4}$$

After the linearization method, two different implicit finite difference schemes with different accuracies are applied to numerically solve (5.4). In (5.5), a first-order accurate backward finite difference scheme was used for temporal discretization. Additionally, for the epsilon term and the last term in the same equation, a second-order accurate central differencing scheme was employed.

$$\begin{aligned} \frac{1}{\Delta t^2}\left(v_i^{j+3} - 2v_i^{j+2} + v_i^{j+1}\right) =& \frac{1}{\Delta x^2}\left(v_{i+1}^{j+1} - 2v_i^{j+1} + v_{i-1}^{j+1}\right) \\ &+ \frac{\varepsilon}{\Delta x^2 \Delta t^2}\left[\left(v_{i+1}^{j+3} - 2v_i^{j+3} + v_{i-1}^{j+3}\right)\right. \\ &\left. - \left(2v_{i+1}^{j+2} - 4v_i^{j+2} + 2v_{i-1}^{j+2}\right)\right] \\ &+ \frac{\varepsilon}{\Delta x^2 \Delta t^2}\left(v_{i+1}^{j} - 2v_i^{j} + v_{i-1}^{j}\right) + s^{j+2}\tilde{f}^{j+2}. \end{aligned} \tag{5.5}$$

To achieve higher accurate in solving (5.4), a second-order accurate backward finite difference scheme was used for temporal discretization in (5.5). Similarly, for the

epsilon term and the last term in the same equation, a fourth-order accurate central differencing scheme was employed.

(5.6)
$$\begin{aligned}\frac{1}{\Delta t^2}\left(2v_i^{j+3}-5v_i^{j+2}+4v_i^{j+1}-v_i^j\right) =&\frac{1}{12\Delta x^2}\left(v_{i+2}^{j+3}+16v_{i+1}^{j+3}-30v_i^{j+3}+16v_{i-1}^{j+3}-v_{i-2}^{j+3}\right)\\ &+\frac{\varepsilon}{16\Delta x^2\Delta t^2}\left[\left(v_{i+2}^{j+3}-2v_i^{j+3}+v_{i-2}^{j+3}\right)\right.\\ &\left.-\left(2v_{i+2}^{j+1}-4v_i^{j+1}+2v_{i-2}^{j+1}\right)\right]\\ &+\frac{\varepsilon}{16\Delta x^2\Delta t^2}\left(v_{i+2}^{j-1}-2v_i^{j-1}+v_{i-1}^{j-1}\right)+s^{j+2}\tilde{f}^{j+2}.\end{aligned}$$

For the numerical procedure, the initial condition is defined as $v_i^0=\varphi_i$, And periodic boundary conditions are defined with combination of Dirichlet and Neumann boundary conditions. In practice, periodic boundary conditions are commonly employed to avoid solving repetitive regions within the computational domain. As a result, fewer numerical grid points are required, and the numerical solution can be obtained with reduced computational cost and time. Moreover, as indicated in (2.3), when periodic boundary conditions are applied, both the function values and the corresponding first-order spatial derivatives at the boundary points are equal. The equations given below satisfy the conditions

$$v_1^j=v_{Nx}^j,\quad v_{Nx}^j=\frac{v_2^j+v_{Nx-1}^j}{2}.$$

The equation solved in this study involves mixed spatial-temporal derivative terms. Accordingly, under periodic boundary conditions, both the second-order spatial derivative and the mixed space-time derivative attain identical values at the boundary points. This aspect has been carefully considered in the numerical example used in the present study.

The computational domain size is $[0,\pi]\times[0,T]$ for space and time. Computational domain is discretized as $x_i=i\,(\Delta x-1)$, $i=1,2,\ldots,Nx$, for spaces, and as $t_j=j\Delta t$ and $j=1,2,\ldots,Nt$ for time. Here the space in x direction exhibits as $\Delta x=\pi/Nx$ and the time step represents as $\Delta t=T/Nt$. Additionally, here Nx and Nt are two positive integers. The value v, φ and f represents with notation about discretization as $v_i^j=v\,(x_i,t_j)$, $\varphi_i=\varphi\,(x_i)$, $\tilde{f}^{j+2}=f\,(x_i,t_{j+2})$, respectively. The initial time $t=0$, represents the initial condition and compatibility requirements. In our numerical computation, $j+3$. represents the present time, $j+2$ signifies the time just prior to the present, $j+1$. denotes the time two steps prior to the present, and finally, j represents the time three steps prior to the present. To ascertain the inverse coefficient $s\,(t)$, we integrate (5.1) over the range from 0 to ϕ with respect to x, incorporating (5.3) and (5.4), resulting in

$$s\,(t)=\frac{E''\,(t)-\varepsilon\left[\pi v_{xtt}\,(\pi,t)-v_{tt}\,(\pi)+v_{tt}\,(0)\right]-\pi v_x\,(\pi,t)}{\int\limits_0^\pi x\tilde{f}\,(x,t)\,dx}. \tag{5.7}$$

The individual discretization of the elements constituting (5.7) using finite differences one by one for (5.5) are given below

$$E''(t) = \left[\left(E^{j+2} - 2E^{j+1} + E^{j}\right)/\Delta t^2\ \right], \tag{5.8}$$

$$v_{tt}(\pi) = \left(\left(v_{Nx}^{j+2} - 2v_{Nx}^{j+1} + v_{Nx}^{j}\right)/\Delta t^2\ \right), \tag{5.9}$$

$$v_{tt}(0) = \left(\left(v_{1}^{j+2} - 2v_{1}^{j+1} + v_{1}^{j}\right)/\Delta t^2\ \right), \tag{5.10}$$

$$\pi v_x(\pi, t) = \pi\left(v_{Nx}^{j+2} - v_{Nx-1}^{j+2}\right)/\Delta x\ . \tag{5.11}$$

First order accurate backward finite difference schemes have been used for (5.8)–(5.11). With the same manner, for (5.6), the individual discretization of the elements constituting (5.7) using finite differences one by are given below

$$E''(t) = \left[\left(2E^{j+2} - 5E^{j+1} + 4E^{j} - E^{j-1}\right)/\Delta t^2\ \right], \tag{5.12}$$

$$v_{tt}(\pi) = \left(\left(2v_{Nx}^{j+2} - 5v_{Nx}^{j+1} + 4v_{Nx}^{j} - v_{Nx}^{j}\right)/\Delta t^2\ \right), \tag{5.13}$$

$$v_{tt}(0) = \left(\left(2v_{1}^{j+2} - 5v_{1}^{j+1} + 4v_{1}^{j} - v_{1}^{j}\right)/\Delta t^2\ \right), \tag{5.14}$$

$$\pi v_x(\pi, t) = \pi\left(3v_{Nx}^{j+2} - 4v_{Nx-1}^{j+2} + 4v_{Nx-2}^{j+2}\right)/2\Delta x. \tag{5.15}$$

Second-order accurate backward finite difference schemes have been used for (5.12)–(5.15). The terms commonly used for the discretization of (5.7) for (5.5) and (5.6) are shown below

$$\pi v_{xtt}(\pi, t) = \pi\left(\left(\left(v_{i+1}^{j+2} - 2v_{i+1}^{j+1} + v_{i+1}^{j}\right) - \left(v_{i}^{j+2} - 2v_{i}^{j+1} + v_{i}^{j}\right)\right)/\Delta x \Delta t^2\ \right). \tag{5.16}$$

The mixed derivative used in (5.16) is discretized using a first-order accurate backward finite difference method

$$\left(\tilde{f}in\right)^{j+2} = \int_0^{\pi} x\tilde{f}(x, t)\, dx. \tag{5.17}$$

To compute (5.17), trapezoidal rule for integration is employed. The value of Nx utilized for numerical solutions differs from the value of Nin used for the trapezoidal rule integration.

In calculating the value of the inverse coefficient in the initial time steps, the initial value of w is utilized, but the detailed discretization is not shown here to avoid excessive detail.

For the numerical solution of (5.5) and (5.6), no iterative methods were employed, a direct method was used instead. The right-hand side matrix, known from previous time steps and used in the direct method, differs for (5.5) and (5.6). For (5.5), the right-hand side matrix used is

$$\begin{aligned} rhs_i = &- 2v_i^{j+2} + v_i^{j+1} + \frac{2\varepsilon}{\Delta x^2}\left(v_{i+1}^{j+2} - 2v_i^{j+2} + v_{i-1}^{j+2}\right) \\ &- \frac{\varepsilon}{\Delta x^2}\left(v_{i+1}^{j+1} - 2v_i^{j+1} + v_{i-1}^{j+1}\right) - s^{j+2}\tilde{f}^{j+2}\Delta t^2. \end{aligned}$$

For (5.6), the right-hand side matrix used is

$$rhs_i = -5v_i^{j+2} + 4v_i^{j+1} - v_i^j + \frac{\varepsilon}{8\Delta x^2}\left(v_{i+2}^{j+1} - 2v_i^{j+1} + v_{i-2}^{j+1}\right) - \frac{\varepsilon}{16\Delta x^2}\left(v_{i+2}^{j-1} - 2v_i^{j-1} - v_{i-2}^{j-1}\right) - s^{j+2}\widetilde{f}^{j+2}\Delta t^2.$$

The implicit finite difference schemes are unconditionally stable; therefore, no restrictive condition is imposed on Δt, Δx, or ε. The schemes remain stable for all positive values of the discretization parameters. However, the choice of Δt affects the accuracy of the numerical solution, particularly for larger values of ε.

6. Numerical Example

Considering inverse problem

$$f(x,t,w) = we^{t^2}\sin 2x, \quad \varphi(x) = \sin 2x, \quad E(t) = -\frac{\pi}{2}e^{t^2},$$

in $x \in [0,\pi]$, $t \in [0,T]$. In that case, the problem transforms as

$$\begin{aligned} &w_{tt} - \varepsilon w_{xxtt} - w_{xx} = s(t)e^{t^2}\sin 2x, \\ &w(x,0) = \sin 2x, \quad x \in [0,\pi], \\ &w(0,t) = w(\pi,t), \quad w_x(0,t) = w_x(\pi,t), \quad 0 \le t \le T, \\ &\int_0^\pi xw(x,t)dx = -\frac{\pi}{2}e^{t^2}. \end{aligned}$$

The analytical solution of this problem can be defined as

$$\{s(t), w(x,t)\} = \left\{\left(6 + 8\varepsilon + 4t^2 + 16\varepsilon t^2\right), e^{t^2}\sin 2x\right\}.$$

6.1. **Grid Independence Study and Time Step Size Determination.** Seven different grid densities are used to determine the grid resolution that guarantees grid independence. The used grid numbers are 20, 40, 80, 160, 320, 640, and 1280. Additionally, five different time steps are used to determine the time step. These are 0.01s, 0.005s, 0.0025s, 0.00125s, and 0.000625s. Both the grid independence study and the time step determination study are conducted separately for both (5.5) and (5.6).

Figure 1 shows separate grid independence studies for (5.5) at five different time steps. The value of $w(x,t)$ decreases as the mesh number increases for all time steps; however, there is little difference between the w values at 640 mesh number and 1280 mesh number. Therefore, the mesh number of 640 is considered as the grid independent mesh number.

After determining the grid independent number as 640 for (5.5), solutions are obtained for the previously specified five different time steps at this mesh number. These solutions are depicted in Figure 2. Upon examining figure 2, it is observed that the solution does not change for time steps of 0.0025s and smaller. For the solution of (5.5), a mesh number of 640 and a time step of 0.0025s are used.

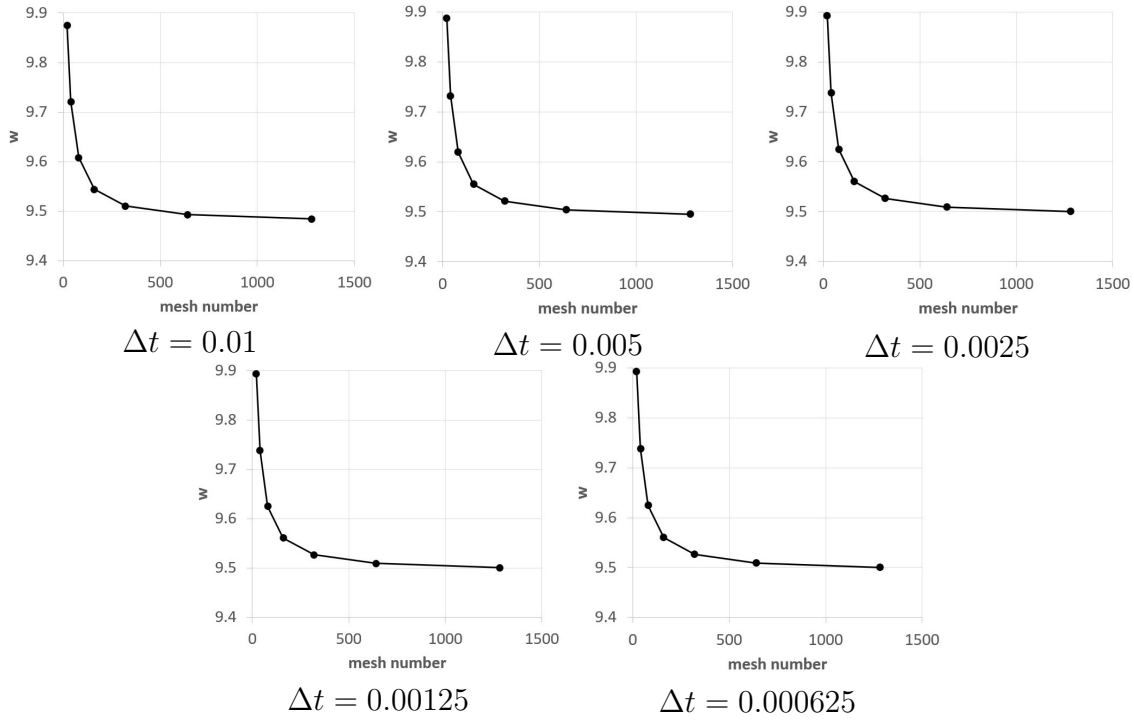

FIGURE 1. Grid independence mesh study for (5.5)

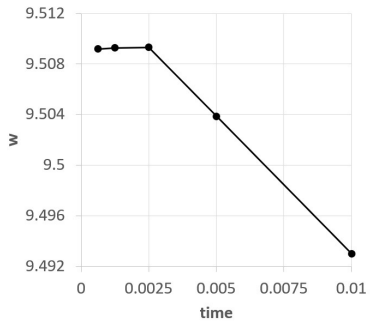

FIGURE 2. Time step size determination for (5.5)

Similar to what is done for (5.5), separate grid independence studies are conducted for (5.6) at five different time steps. This study is illustrated in Figure 3. The value of $w(x,t)$ decreases as the mesh number increases for all time steps, but there is little difference between the u values at 640 mesh number and 1280 mesh number. Therefore, the mesh number of 640 is considered as the grid independent mesh number for (5.6).

After determining the grid-independent number as 640 for (5.6), solutions are obtained for the previously specified five different time steps at this grid number. These solutions are depicted in Figure 4. According to Figure 4, it is observed that

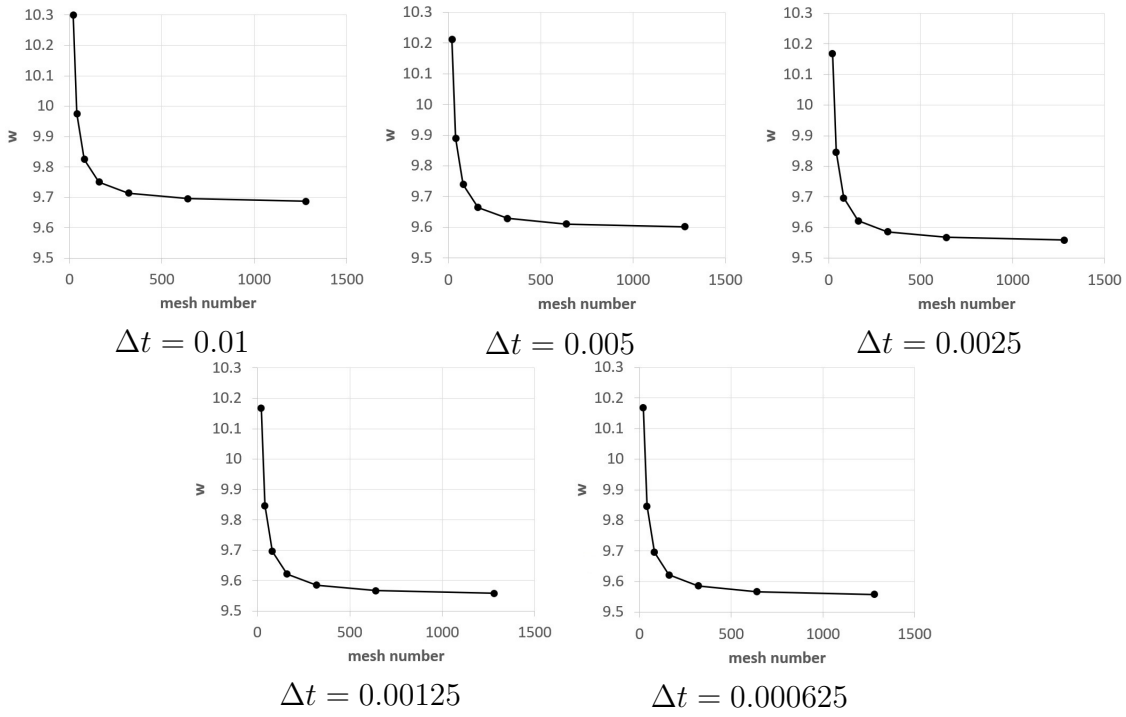

FIGURE 3. Grid independence mesh study for (5.6)

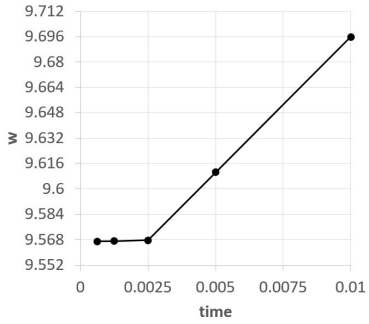

FIGURE 4. Time step size determination for (5.6)

the solution does not change for time steps of 0.025s and smaller. For the solution of (5.5), a mesh number of 640 and a time step of 0.0025s are used.

6.2. **Inverse Coefficient.** The value of Nin used to compute the integral in (5.17) is set to 1000 for all solutions, independent of the numerical grid. Figure 5 shows (a) the time-dependent variation of the inverse coefficient, (b) the time-dependent variation of the true error for the inverse coefficient, and (c) the time-dependent variation of the absolute relative error for the inverse coefficient. According to figure 5a, it can be observed that the inverse coefficient increases over time. The exact solution and two different numerical solutions appear very close to each other.

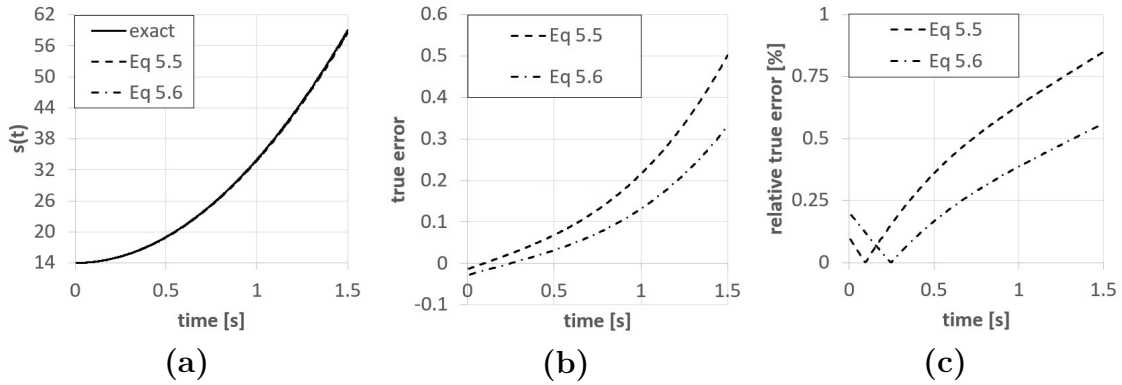

FIGURE 5. (a) Inverse coefficient variation, (b) true error variation, and (c) absolute relative error variation with time

The true errors of the two numerical solutions increase over time, as shown in figure 5b. (5.6), which has a higher accuracy, is closer to the exact solution. The absolute relative error reveals the discrepancies between the exact solution and the numerical solution. When looking at figure 5c, it can be observed that for both numerical solutions, the absolute relative error initially decreases over time and reaches zero error. However, after this point, the absolute error increases over time. Similarly, the equation with a more accurate finite difference scheme, (5.6), produces results closer to the exact solution. The absolute relative errors for both numerical solutions do not exceed 1%.

6.3. **Values of** $w(x,t)$**.** Figure 6 illustrates the time-dependent variation of the w value obtained from three different approaches: (a) the exact solution, (b) the numerical solution computed using (5.5), and (c) the numerical solution obtained from (5.6). At a specific instant in time, the solution profile exhibits a hyperbolic-type curve characterized by two distinct peaks: one positive and one negative. These peaks represent the oscillatory nature of the wave equation and indicate the propagation of wave energy in opposite directions. As time progresses, the amplitudes of these peaks increase gradually, reflecting the dynamic behavior of the solution and the growth of the wave structure over time. A comparison of the three subfigures demonstrates that the numerical results produced by (5.5) and (5.6) closely follow the behavior of the exact solution. The spatial distribution, peak locations, and overall shape of the surfaces are nearly identical in all three cases. This strong agreement indicates that the proposed numerical schemes are capable of accurately capturing the temporal evolution and spatial characteristics of the solution. Minor discrepancies, if present, remain negligible and do not significantly affect the overall solution structure.

Figure 7 presents the time-dependent distribution of the true error between the exact solution and the numerical solutions obtained using two different numerical schemes: (a) the numerical solution computed according to (5.5) and (b) the numerical solution computed according to (5.6). From the figure, it can be clearly observed that the

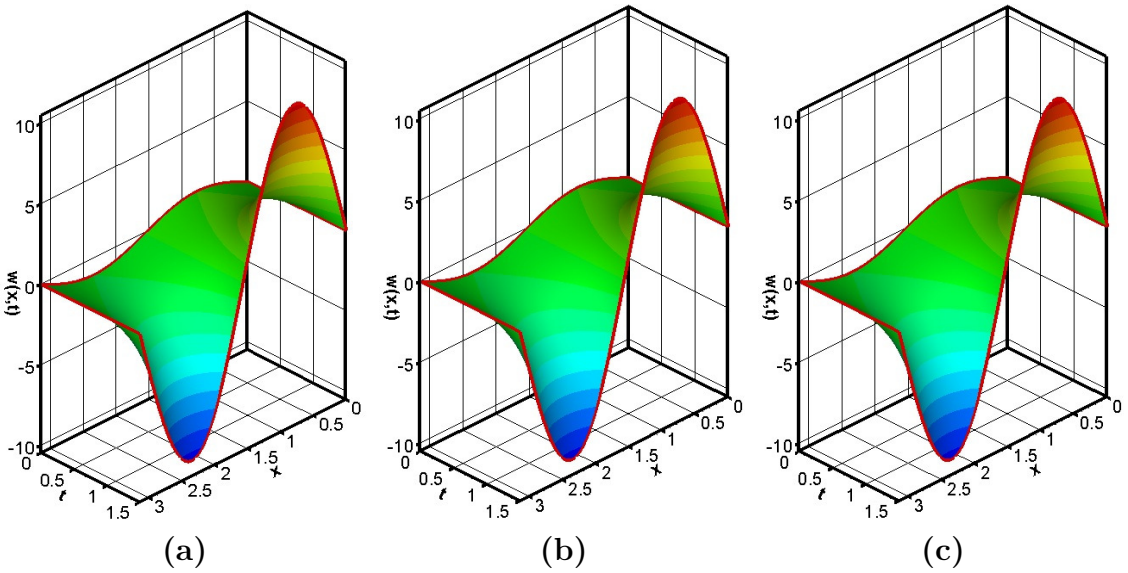

FIGURE 6. w value variation with time for (a) exact solution, (b) for numerical solution of (5.5) and (c) for numerical solution of (5.6)

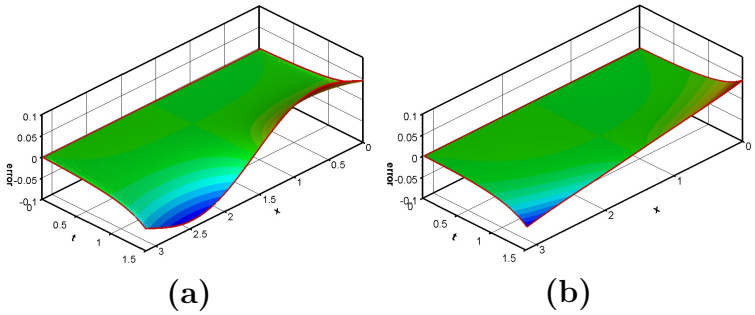

FIGURE 7. True error variation with time for (a) numeric solution of (5.5) and (b) numeric solution of (5.6)

magnitude of the true error is generally more pronounced near the boundaries of the computational domain. In contrast, the central region of the domain exhibits very small error values, indicating that both numerical schemes capture the core structure of the solution with a high level of accuracy. This behavior is typical in numerical approximations, where boundary treatments and discretization effects may lead to slightly larger deviations near the domain limits. A comparison between the two subfigures further reveals that the fourth-order accurate scheme given by (5.6) produces smaller error magnitudes compared to the second-order accurate scheme described by (5.5). The smoother error surface and reduced amplitude of the error in Figure 7(b) demonstrate the improved accuracy of the higher-order scheme. This result confirms that increasing the order of accuracy enhances the capability of the numerical method to approximate the exact solution more precisely.

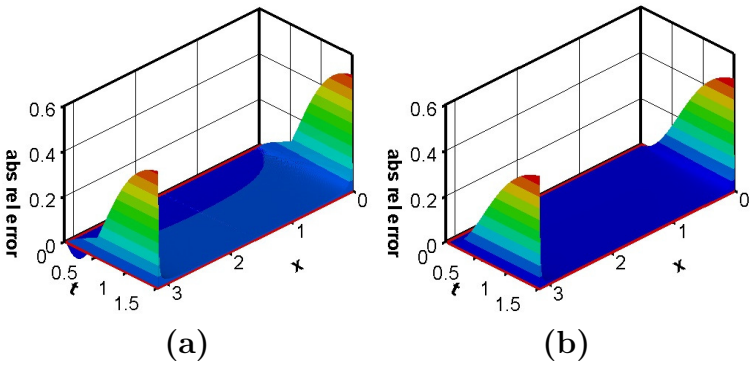

FIGURE 8. Absolute relative true error variation with time for (a) numeric solution of (5.5) and (b) numeric solution of (5.6)

Figure 8 illustrates the time-dependent variation of the absolute relative true error between the exact solution and the numerical solutions obtained using two different numerical schemes: (a) the numerical solution based on (5.5) and (b) the numerical solution based on (5.6). From the figure, it can be observed that the absolute relative true errors for both numerical schemes tend to increase near the boundary points of the computational domain. This behavior is commonly encountered in numerical simulations, where boundary treatments and discretization effects may slightly influence the accuracy of the solution near the edges of the domain. In contrast, the interior region of the domain exhibits very small error values, indicating that the numerical schemes approximate the exact solution with high accuracy across most of the computational region. Despite the slight increase near the boundaries, the absolute relative errors remain below 1% for both numerical solutions, demonstrating the overall reliability and stability of the proposed numerical methods. A comparison of Figures 8(a) and 8(b) further reveals that the higher-order accurate scheme given by (5.6) produces smaller error magnitudes than the second-order accurate scheme described by (5.5). The error surface in Figure 8(b) appears smoother and closer to zero over a larger portion of the domain, highlighting the improved accuracy achieved by the higher-order formulation. These observations are consistent with the results obtained from the inverse coefficient analysis (Figure 5(c)) and the true error analysis (Figure 7), where the higher-order scheme also demonstrated superior performance. Therefore, the results presented in Figure 8 further confirm that increasing the order of accuracy significantly enhances the numerical solution's ability to approximate the exact solution with greater precision, which is the expected outcome in numerical analysis.

7. CONCLUSIONS

Analytical and numerical investigations have been conducted for one dimensional nonlinear pseudo-hyperbolic equation involving time-dependent inverse coefficient with periodic boundary conditions. To obtain an analytical solution, we employ

the generalized Fourier method for calculating Fourier coefficients. Furthermore, an iterative approach is utilized to ensure convergence while evaluating the uniqueness and stability of the solution for the nonlinear problem. Moreover, to numerically address the one-dimensional pseudo hyperbolic problem with transient inverse coefficient, we propose the use of the implicit Finite Difference Method. Two finite difference equations are developed and solved with varying accuracies. In the first equation (5.5), a first-order accurate time discretization is implemented, and second-order accurate finite difference equations are utilized for the discretization of spatial and multi-variable partial differential equations. In the second equation (5.6), a second-order accurate time discretization is applied, and fourth-order accurate finite difference equations are employed for the discretization of spatial and multi-variable partial differential equations. Grid independence and time determination stud is done for both (5.5) and (5.6). The major conclusions are listed below.

- Mesh number of 640 and time step size of 0.0025s are determined for both finite differences scheme with different accuracies.
- The inverse coefficient increases over time in both exact and numerical computations
- An equation with a more accurate finite difference scheme estimates results closer to the exact solution of the inverse coefficient.
- At a particular point in time, the solution of the pseudo-hyperbolic problem with inverse coefficient exhibits curve with two peaks, one positive and one negative. Over time, these two peaks gradually increase in magnitude.
- The more accurate finite difference equation is successful in predicting the pseudo-hyperbolic curve, but the difference between the two finite difference equations is not significant.

References

[1] B. Epstein, *Partial Differential Equations*, 1st ed., McGraw-Hill Book Company Inc., New York, 1962.
[2] W. A. Strauss, *Partial Differential Equations*, 2nd ed., Wiley, USA, 2008.
[3] J. Marazzani, N. Cavalagli and V. Gusella, *Elastic properties estimation of masonry walls through the propagation of elastic waves: An experimental investigation*, Appl. Sci. **11**(19) (2021), Article ID 9091. https://doi.org/10.3390/app11199091
[4] D. Y. Tzou, *Resonance phenomenon in thermal waves*, Internat. J. Engrg. Sci. **29**(9) (1991), 1167–1177. https://doi.org/10.1016/0020-7225(91)90119-N
[5] L. E. Kinsler, A. R. Frey, A. B. Coppens and J. V. Sanders, *Fundamentals of Acoustics*, 4th ed., Wiley, Weinheim, 2000.
[6] W. J. Smith, *Modern Optical Engineering*, 3rd ed., McGraw-Hill, New York, 2001.
[7] D. C. Karnoop, D. L. Margolid and R. C. Rosenberg, *System Dynamics: Modeling, Simulation, and Control of Mechatronic Systems*, 5th ed., Wiley, New Jersey, 2012.
[8] M. Hamidaoui, C. Shao and S. A. Haouassi, *PD-type iterative learning control algorithm for one-dimensional linear wave equation*, International Journal of Control Automation Systems **18** (2020), 1045–1052.

[9] M. M. Lavrentiev, *Some Improperly Ill-Posed Problems of Mathematical Physics*, 1st ed., Springer, Berlin, 1967.
[10] O. M. Alifanov, E. A. Artyukhin and S. V. Rumyantsev, *Extreme Methods for Solving Ill-Posed Problems with Applications to Inverse Problems*, Begell House Inc., New York, 1995.
[11] H. W. Engl, M. Hanke and A. Neubauer, *Regularization of Inverse Problems*, 1st ed., Springer, Netherlands, 1996.
[12] V. G. Romanov, *Inverse Problems of Mathematical Physics*, 1st ed., VNU Science Press BV, Utrecht, 1987.
[13] V. G. Romanov, *Investigation Methods for Inverse Problems*, 1st ed., VSP, Utrecht, 2002.
[14] V. Isakov, *Inverse Problems in Partial Differential Equations*, 2nd ed., Springer, New York, 1998.
[15] S. I. Kabanikhin and A. Lorenzi, *Identification Problems of Wave Phenomena*, 1st ed., VSP, Utrecht, 1999.
[16] M. M. Lavrentiev and V. G. Romanov, *Ill-Posed Problems of Mathematical Physics and Analysis*, American Mathematical Society, Moscow, 1986.
[17] I. Baglan, *Determination of a coefficient in a quasilinear parabolic equation with periodic boundary condition*, Inverse Problems in Science & Engineering **23**(5) (2015), 884–900. https://doi.org/10.1080/17415977.2014.947479
[18] G. W. Hill, *On the part of the motion of the lunar perigee which is a function of the mean motions of the sun and moon*, Acta Math. **8** (1886), 1–36.
[19] J. W. Brown and R. V. Churchill, *Fourier Series and Boundary Value Problems*, 5th ed., McGraw-Hill Education, New York, 1993.
[20] G. D. Smith, *Numerical Solution of Partial Differential Equations: Finite Difference Methods*, 3rd ed., Clarendon Press, New York, 1985.
[21] K. W. Morton and D. F. Mayers, *Numerical Solution of Partial Differential Equations*, 2nd ed., Cambridge University, Cambridge, 2005.
[22] V. G. Dmitriev, A. N. Danilin, A. R. Popova and N. V. Pshenichnova, *Numerical analysis of deformation characteristics of elastic inhomogeneous rotational shells at arbitrary displacements and rotating angles*, Computation **10**(10) (2022), Article ID 184. https://doi.org/10.3390/computation10100184
[23] A. C. Benim and W. Zinser, *Investigation into finite element analysis of confined turbulent flows using a k-ϵ model of turbulence*, Computer Methods in Applied Mechanics and Engineering **51**(1–3) (1985), 507–523. https://doi.org/10.1016/0045-7825(85)90045-3
[24] A. C. Benim, *Finite element analysis of confined turbulent swirling flows*, Internat. J. Numer. Methods Fluids **11**(6) (1990), 697–717. https://doi.org/10.1002/fld.1650110602
[25] A. C. Benim and W. Zinser, *A segregated formulation of Navier-Stokes equations with finite elements*, Computer Methods in Applied Mechanics and Engineering **57**(2) (1986), 223–237. https://doi.org/10.1016/0045-7825(86)90015-0
[26] H. K. Versteeg and W. Malalasekera, *An Introduction to Computational Fluid Dynamics*, 2nd ed., Pearson, Prentice Hall, London, 2007.
[27] J. L. Xia, B. L. Smith, A. C. Benim, J. Schmidli and G. Yadigaroglu, *Effect of inlet and outlet boundary conditions on swirling flows*, Computers & Fluids **26**(8) (1997), 811–823. https://doi.org/10.1016/S0045-7930(97)00026-1
[28] S. Bhattacharyya, A. C. Benim, H. Chattopadhyay and A. Banerjee, *Experimental and numerical analysis of forced convection in a twisted tube*, Thermal Science **23**(4) (2019), 1043–1052. https://doi.org/10.2298/TSCI19S4043B
[29] S. Bhattacharyya, A. C. Benim, M. Pathak, S. Chamoli and A. Gupta, *Thermohydraulic characteristics of inline and staggered angular cut baffle inserts in the turbulent flow regime*, Journal of Thermal Analysis & Calorimetry **140** (2020), 1519–1536. https://doi.org/10.1007/s10973-019-09094-8

[30] N. Biswas, N. K. Manna, A. Datta, D. K. Mandal and A. C. Benim, *Role of aspiration to enhance MHD convection in protruded heater cavity*, Prog. Comput. Fluid Dyn. **20**(6) (2020), 363–378. https://doi.org/10.1504/PCFD.2020.111408

[31] A. C. Benim, M. Diederich and B. Pfeiffelmann, *Aerodynamic optimization of airfoil profiles for small horizontal axis wind turbines*, Computation **6**(2) (2018), Article ID 34. https://doi.org/10.3390/computation6020034

[32] R. A. Damseh, M. S. Tahat and A. C. Benim, *Nonsimilar solutions of magnetohydrodynamic and thermophoresis particle deposition on mixed convection problem in porous media along a vertical surface with variable wall temperature*, Prog. Comput. Fluid Dyn. **9**(1) (2009), 58–65. https://doi.org/10.1504/PCFD.2009.022309

[33] L. Anné, P. Joly and Q. H. Tran, *Construction and analysis of higher order finite difference schemes for the* $1D$ *wave equation*, Comput. Geosci. **4**(3) (2020), 207–249.

[34] S. Wang, A. Nissen and G. Kreiss, *Convergence of finite difference methods for the wave equation in two space dimensions*, Mathematics Computation **87**(314) (2018), 2737–2763. http://dx.doi.org/10.1090/mcom/3319

[35] J. Liu and B. Z. Guo, *A new semidiscretized order reduction finite difference scheme for uniform approximation of one-dimensional wave equation*, SIAM J. Control Optim. **58**(4) (2020), 2256–2287. https://doi.org/10.1137/19M1246535

[36] M. E. U. Madaliev, Z. E. Abdulkhaev, N. E. Toshpulatov and A. A. Sattorov, *Comparison of finite-difference schemes for the first-order wave equation problem*, AIP Conference Proceedings **2637**(1) (2022), Article ID 040022. https://doi.org/10.1063/5.0119158

[37] A. G. da Silva Jr, J. A. Martins and E. C. Romao, *Numerical simulation of a one-dimensional non-linear wave equation*, Engineering, Technology & Applied Science Research **12**(3) (2022), 8574–8577. https://doi.org/10.48084/etasr.4920

[38] M. J. Huntul, I. Tekin, M. K. Iqbal and M. Abbas, *An inverse problem of recovering the heat source coefficient in a fourth-order time-fractional pseudo-parabolic equation*, J. Comput. Appl. Math. **441** (2024), Article ID 115712. https://doi.org/10.1016/j.cam.2023.115712

[39] M. J. Huntul, Kh. Khompysh, M. K. Shazyndayeva and M. K. Iqbal, *An inverse source problem for a pseudoparabolic equation with memory*, AIMS Math. **9**(6) (2024), 14186–14212. https://doi.org/10.3934/math.2024689

[40] Kh. Khompysh, M. J. Huntul, M. K. Shazyndayeva and M. K. Iqbal, *An inverse problem for pseudoparabolic equation: existence, uniqueness, stability, and numerical analysis*, Quaest. Math. **47**(10) (2024), 1979–2001. https://doi.org/10.2989/16073606.2024.2347432

[41] M. J. Huntul, I. Tekin, M. K. Iqbal and M. Abbas, *An inverse problem of reconstructing the unknown coefficient in a third-order time fractional pseudoparabolic equation*, An. Univ. Craiova Ser. Mat. Inform. **51**(1) (2024), 54–81. https://doi.org/10.52846/ami.v51i1.1744

[1]Department of Mathematics,
Kocaeli University,
41380 Kocaeli, Turkey
Email address: akbala.yernazar@kocaeli.edu.tr
ORCID iD: https://orcid.org/0000-0002-0068-4954
Email address: isakinc@kocaeli.edu.tr
ORCID iD: https://orcid.org/0000-0003-4900-6027

[2]Department of Mechanical Engineering,
Kocaeli University,
41380 Kocaeli, Turkey
Email address: erman.aslan@kocaeli.edu.tr
ORCID iD: https://orcid.org/0000-0001-8595-6092

*Corresponding Author